Copyright Warning & Restrictions

The copyright law of the United States (Title 17, United States Code) governs the making of photocopies or other reproductions of copyrighted material.

Under certain conditions specified in the law, libraries and archives are authorized to furnish a photocopy or other reproduction. One of these specified conditions is that the photocopy or reproduction is not to be "used for any purpose other than private study, scholarship, or research." If a, user makes a request for, or later uses, a photocopy or reproduction for purposes in excess of "fair use" that user may be liable for copyright infringement,

This institution reserves the right to refuse to accept a copying order if, in its judgment, fulfillment of the order would involve violation of copyright law.

Please Note: The author retains the copyright while the New Jersey Institute of Technology reserves the right to distribute this thesis or dissertation

Printing note: If you do not wish to print this page, then select "Pages from: first page # to: last page #" on the print dialog screen

NJIT
New Jersey's Science & Technology University

The Van Houten library has removed some of the personal information and all signatures from the approval page and biographical sketches of theses and dissertations in order to protect the identity of NJIT graduates and faculty.

ABSTRACT

LOW PRESSURE CHEMICAL VAPOR DEPOSITION OF SILICON CARBONITRIDE FILMS FROM TRI(DIMETHYLAMINO)SILANE

by
Rajive Shah

A literature study to investigate the incorporation of silicon into SiC and Si_3N_4 films from various organosilanes was carried out. The Arrhenius activation energy for the synthesis of silicon, silicon carbide and silicon nitride films from various organosilanes range from 165-210 kJ/mol. A review of recent studies have indicated that silicon deposition is the rate determining step in the synthesis of silicon from silane. It is proposed here that this hypothesis can be established for the synthesis of silicon carbide, silicon nitride and silicon carbonitride film. Limited experiments indicated that the silicon deposition is a rate determining step in the deposition of silicon carbonitride films from tri(dimethylamino)silane (TDMAS).

The deposition of Si-C-N film is found to be consistent with an activation energy of 175 kJ/mol in the temperature range of 650-750°C. The film composition, its refractive index, density, IR spectroscopy and the Young's Modulus is determined. A complete study on the deposition of silicon carbonitride film can be carried out for further conformance.

Blank Page

LOW PRESSURE CHEMICAL VAPOR DEPOSITION OF SILICON CARBONITRIDE FILMS FROM TRI(DIMETHYLAMINO)SILANE

by
Rajive Shah

A Thesis
Submitted to the Faculty of
New Jersey Institute of Technology
in Partial Fulfillment of the Requirements for the Degree of
Master of Science in Chemical Engineering

Department of Chemical Engineering, Chemistry, and Environmental Science

May 1997

Blank Page

APPROVAL PAGE

LOW PRESSURE CHEMICAL VAPOR DEPOSITION OF SILICON CARBONITRIDE FILMS FROM TRI(DIMETHYLAMINO)SILANE

Rajive Shah

5/1/97

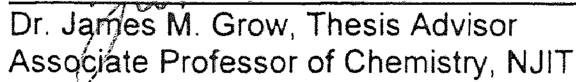

Dr. James M. Grow, Thesis Advisor — Date
Associate Professor of Chemistry, NJIT

5/1/97

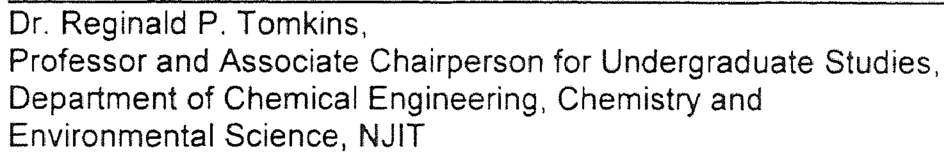

Dr. Reginald P. Tomkins, — Date
Professor and Associate Chairperson for Undergraduate Studies,
Department of Chemical Engineering, Chemistry and
Environmental Science, NJIT

5/1/97

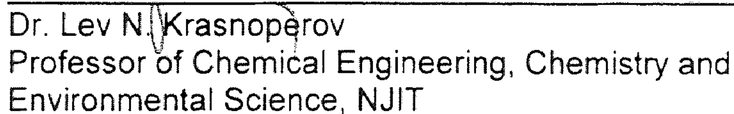

Dr. Lev N. Krasnoperov — Date
Professor of Chemical Engineering, Chemistry and
Environmental Science, NJIT

Blank Page

BIOGRAPHICAL SKETCH

Author: Rajive Shah

Degree: Master of Science

Date: May 1997

Date of Birth:

Place of Birth:

Undergraduate and Graduate Education:

- Master of Science in Chemical Engineering,
  New Jersey Institute of Technology,
  Newark, New Jersey, 1997

- Bachelor of Engineering in Chemical Engineering,
  Bombay University,
  Bombay, India, 1995

Major: Chemical Engineering

Presentations and Publications:

Shah, R., K., "Glass Lined Equipments in Chemical Industries and Their Accessories." *Chemical Weekly*, Bombay, India, 20 September 1994.

This thesis is dedicated to
my family

ACKNOWLEDGMENT

The author expresses his sincere gratitude to his advisor, Professor James M. Grow for his guidance, inspiration, and support throughout this research, without which it would not have been completed.

Special thanks to Professor Reginald P. Tomkins and Professor Lev N. Krasnoperov for serving as members of the thesis review committee.

The author appreciates the timely help and suggestion from the CVD laboratory members, including: Dr. Roland Levy, Vitaly Sigal, Dr. Jan Opyrchal, Mahalingam Bhaskaran, Dr. Romiana Petrova, Muhammad Hussain, Krit Aryusook and Ramanuja Narahari.

TABLE OF CONTENTS

Chapter | Page

1 REVIEW OF CVD 1

1.1 Introduction 1

1.2 Fundamental Aspects of CVD 3

1.3 Thermodynamics of CVD 4

1.4 Kinetics and Mass Transport Mechanism 6

1.4.1 Deposition Sequence 6

1.4.2 Diffusion 8

1.4.3 Rate Limiting Steps 9

1.4.4 Reactant Gas Concentration and Velocity 12

1.5 Advantages of CVD 14

1.6 Limitations of CVD 15

1.7 Objectives of the Research Work 15

2 LITERATURE REVIEW 17

2.1 Preparation 17

2.2 Properties 17

2.3 Applications 20

2.4 Methods of Thin Film Deposition 21

2.4.1 Physical Vapor Deposition 21

2.4.2 Chemical Vapor Deposition 22

2.5 Types of CVD Processes 23

2.5.1 Thermally Activated CVD 23

2.5.2 Plasma Enhanced Chemical Vapor Deposition (PECVD) 25

2.5.3 Photo-Induced Chemical Vapor Deposition (PHCVD) 26

2.6 Summary 27

TABLE OF CONTENTS (Continued)

Chapter Page

3 EXPERIMENTAL PROCEDURE 28

3.1 LPCVD Reactor 28

3.2 Pre-Deposition Procedure 30

3.2.1 Leak Check 30

3.2.2 Flow Rate Calibration 30

3.3 Deposition Procedure 32

3.3.1 Wafer Loading 32

3.3.2 Film Deposition 33

3.4 Film Characterization Techniques 35

3.4.1 Initial Analysis 35

3.4.2 Refractive Index Measurements 36

3.4.3 Infra Red Spectroscopy 37

3.4.4 Stress Measurements 38

3.4.5 X-ray Diffraction Studies 40

3.4.6 Compositional Analysis 41

3.4.7 Hardness and Young's Modulus Measurements 43

4 LITERATURE REVIEW OF SILICON CARBIDE DEPOSITION 47

4.1 Structure Study 48

4.2 Role of Hydrogen During Deposition 50

4.3 Deposition of Carbon and Silicon Species 54

4.4 Review of Deposition from Silanes 55

4.5 Silicon Carbide Synthesis from Organosilanes 57

5 RESULTS AND CONCLUSIONS 66

5.1 Deposition of Silicon Carbonitride Films 66

TABLE OF CONTENTS
(Continued)

Chapter **Page**

5.2 Characterization Of Silicon Carbonitride Films 69

5.2.1 Film Deposition 69

5.2.2 Density 72

5.2.3 Refractive Index 74

5.2.4 Fourier Transform Infra Red Spectroscopy 75

5.2.5 Young's Modulus of Silicon Carbonitride 78

5.3 Conclusions 80

6 REFERENCES 82

LIST OF TABLES

Table **Page**

2.1 Properties of CVD SiC 19

3.1 Specification of the Si Wafer 34

LIST OF FIGURES

Figure		Page
1.1	Chemical reaction energetics	5
1.2	Forward exothermic reaction greater than reverse endothermic reaction	6
1.3	Sequence of events during deposition	7
1.4	Temperature dependence of growth rate for CVD films	10
1.5	Changes in reactant velocity along a tubular reactor	13
1.6	Changes in reactant concentration along a tubular reactor	14
2.1	Phase diagram of the SiC system	18
3.1	Schematic representation of the LPCVD reactor	29
3.2	Schematic diagram of a typical silicon wafer showing points where thickness was measured	36
5.1	Dependence of growth rate on temperature	68
5.2	ESCA profile of silicon carbonitride film at 750°C, pressure of 0.5 torr and flow rate of 10sccm	70
5.3	ESCA profile of silicon carbonitride film at 700°C, pressure of 0.2 torr and flow rate of 20sccm	71
5.4	Density of silicon carbide at 850°C	73
5.5	FTIR spectrum for silicon carbonitride film at a temperature of 700°C, pressure of 0.2 torr and flow rate of 10 sccm	76
5.6	FTIR spectrum for silicon carbonitride film at a temperature of 700°C, pressure of 0.5 torr and flow rate of 20 sccm	77
5.5	Young's Modulus of silicon carbonitride films at 700°C	78
5.6	Young's Modulus of silicon carbonitride films at 750°C	79
5.7	Young's Modulus of silicon carbonitride films at 850°C	80

CHAPTER 1

REVIEW OF CVD

1.1 Introduction

Chemical vapor deposition (CVD) is defined as the formation of a non-volatile solid film that deposits atomistically on a suitably placed substrate by the reaction of vapor phase chemicals (reactants) that contain the required constituents [1]. It belongs to the class of vapor transfer processes which are atomistic in nature; that is, the deposition species may be atoms or molecules or a combination of these. It has been possible to deposit almost any metal and non-metallic element, including carbon or silicon, as well as compounds such as carbides, nitrides, oxides, intermetallics and others with CVD. This technology has been known in electronics because it provides a means of placing pure and doped materials at specific locations on microcircuits.

CVD reactants have to be handled carefully in semiconductor research where the gases are often phosphoric and toxic. For high temperature solid materials, CVD technologies are desired which do not contain entrapped gases and have high densities, which cannot be usually achieved in low temperature deposits. This area of materials research and development has grown very rapidly in the last twenty years and has applications in diverse technologies such as fabrication of solid state electronic devices semiconductors, optoelectronics, optics, cutting tools, nuclear reactor components and corrosion applications. Chemical vapor deposition is a very versatile process used in the production of

coatings, powders, fibers and monolithic components. It can have a single crystal, polycrystalline or amorphous structure. In addition to its unique versatility, the synthesis and vapor phase growth method of chemically vapor deposited materials can operate efficiently at low temperatures. For example, refractory oxide glasses and metals can be deposited at temperatures of only 300 to 500°C. This feature is very important in advanced VLSI devices with short channel lengths and shallow junctions, where the lateral and vertical diffusion of dopants must be minimized. The short channel lengths and the shallow junctions also help in minimizing process-induced crystallographic damage, wafer warpage and contamination by diffusion of impurities

The wide range of CVD products is related by the following recent commercial products:

- A speaker diaphragm with improved acoustical properties coated with a thin film of diamond can be obtained by means of plasma CVD
- Diamond-like carbon coatings produced by plasma CVD for bushings and textile components with improved wear resistance
- CVD coated titanium carbide and titanium nitride tools greatly outperform uncoated tools and are rapidly taking over the industry
- CVD boron fibers which are extremely stiff and strong are used as reinforcement in structural components of USAF fighter planes
- Remarkable resistance to corrosion in small rocket nozzles at temperatures upto 2000°C can be obtained by depositing metallo-organic CVD

CVD is now truly an international business and no longer a U.S. monopoly. In Japan, in other Pacific Rim countries and in Europe, a great deal of work is under way, in research as well as in production. The U.S. is still in the lead with an estimated 40% of the business, followed by Europe and Japan with 25% each, the balance being for the rest of the world.

1.2 Fundamental Aspects of CVD

The basic types of chemical reactions which occur during CVD include pyrolysis, gas phase decomposition, nitride and carbide formation, synthesis reaction and chemical transport. A sequence of several reaction types may be involved to create a particular end product. The chemical reactions may take place close to the wafer surface (Heterogeneous reaction) or in the gas phase (Homogeneous reaction) leading to the formation of a solid material. Heterogeneous reactions are much more desirable, as such reactions occur selectively on heated surfaces, and produce good quality films. Homogeneous reactions, on the other hand are undesirable, as they form gas phase clusters of the depositing material, which can result in poorly adhering, low density films, or defects in the depositing film. In addition, such reactions also consume reactants and can cause decrease in deposition rates. Thus, one important characteristic of a chemical reaction for CVD application is the degree to which heterogeneous reactions are favored over gas phase reactions.

Volatility requirements dictate that the vapor pressure of the liquid reactants must be sufficiently high (usually when heated) to produce an

adequate quantity of vapor that can be transported by a carrier gas to the reaction chamber. Gaseous reactants, if available, are preferred since they can be readily metered and introduced into the CVD reactor. The vapor pressure of side products must be high to facilitate their elimination from the reactor, whereas the resulting coating product must have a low volatility to remain on the substrate. The reaction energy to activate and drive the chemical process can be thermal, supplied by an electric glow discharge (plasma), or attained by electromagnetic radiation (usually ultraviolet or laser radiation).

1.3 Thermodynamics of CVD

A CVD reaction is governed by *thermodynamics*, that is the driving force which indicates the direction the reaction is going to proceed (if at all) and by *kinetics*, which can determine the rate controlling mechanism. When the gaseous reactants are converted to a solid product, the first step in the theoretical analysis is to determine if the thermodynamics is favorable, that is the free energy change of the reaction, ΔG_r^0 is negative. In order to determine the ΔG_r^0, it is necessary to know the thermodynamic properties of each component, specifically their standard Gibbs free energies of formation, ΔG_f^0. The relationship can be expressed as follows:

$$\Delta G_r^0 = \Sigma \, \Delta G_f^0 \text{ products} - \Sigma \, \Delta G_f^0 \text{ reactants} \qquad (1.1)$$

The free energy of formation is not a fixed value but varies as a function of several parameters which include the type of reactants, the molar ratio of these reactants, and the process temperature. The calculation of the thermodynamic equilibrium of a CVD system can provide useful information on the characteristics and behavior of the reaction including the optimum range of deposition conditions. It is based on the rule of thermodynamics which states that a system will be in equilibrium when the Gibbs free energy is at a minimum. The objective then is the minimization of the total free energy of the system and the calculation of equilibria at constant temperature and pressure [2]. Computer programs such as SOLGASMIX developed by Erikson and Besmann [3,4] are now widely used in the equilibrium calculations in CVD systems.

It is sometimes observed that higher reactor temperature leads to lower film growth rates in gaseous systems. The individual forward and reverse reaction components are shown in the figure1.1 below.

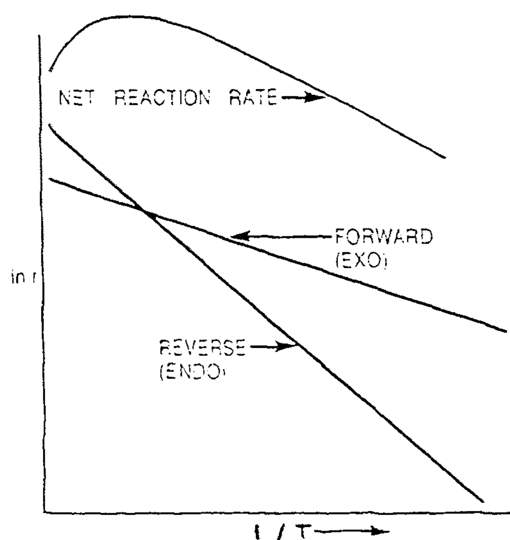

Figure 1.1 Chemical reaction energetics

This can be explained by considering the reversibility of chemical reactions. For exothermic reactions, ΔH° is negative and the reactants have more heat than products. For endothermic reactions, ΔH° is positive. The net reaction rate or difference between the individual rates is also indicated as shown in the figures 1.1 & 1.2. It reaches a maximum and then drops along with the temperature for gaseous systems. The term r represents the rate of reaction.

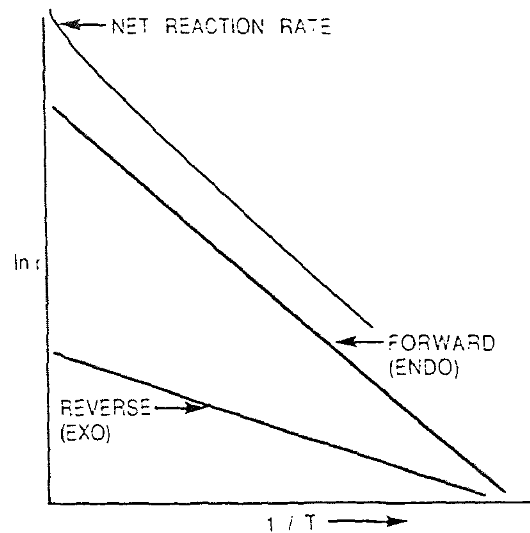

Figure 1.2 Forward exothermic reaction is greater that reverse endothermic reaction

1.4 Kinetics and Mass Transport Mechanism

1.4.1 Deposition Sequence

The sequence of events taking place during a CVD reaction is shown graphically in Figure 1.3 and can be summarized as follows [5]:

1. Arrival of the Reactants

   a) bulk transport of reactants into the chamber,

b) gaseous diffusion of reactants to the substrate surface,

c) adsorption of reactants onto the substrate surface.

2. Surface chemistry

a) surface diffusion of the reactants,

b) surface reaction.

3. Removal of by- products

a) desorption of by-products from the substrate surface,

b) gaseous diffusion of by-products away from the substrate surface,

c) bulk transport of by-products out of the reaction chamber.

These steps occur in the sequence shown and the slowest step will determine the rate. The concept of boundary layer applies in most CVD depositions in the viscous flow range where pressure is relatively high. The viscous flow regime occurs for higher Reynolds number.

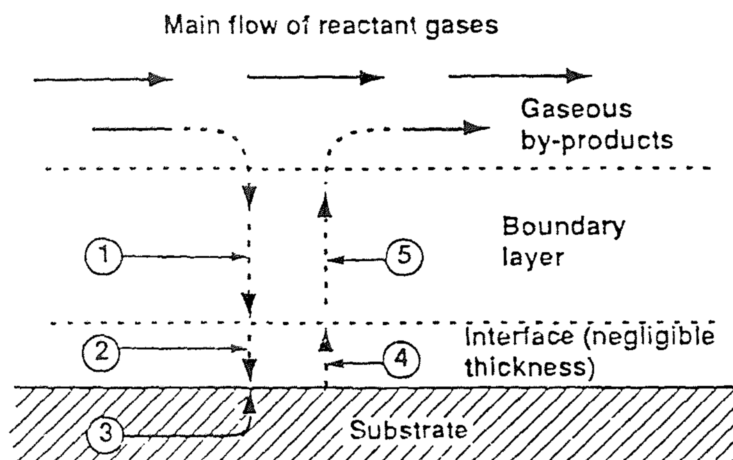

Figure 1.3 Sequence of events during deposition

The Reynolds number (Re) is given by $Re = dv\rho/\mu$

d is the reactor diameter

v is the flow velocity

ρ is the gas density

μ is the viscosity

The flow becomes more viscous for higher values of flow velocity and gas density. In cases of low pressure (i.e. in the mtorr range), the concept is no longer applicable.

1.4.2 Diffusion

The phenomenon of diffusion occurs in gases and liquids as well as in solids. If two different gases are initially separated and then allowed to mix, each will move from regions of higher to lower concentrations, thus increasing the entropy of the system. Thus diffusion (J) may be defined as the migration of an atomic or molecular species within a given matrix under the influence of a concentration gradient. It is characterized by Fick's Law and is given by:

$$J = -D\, dc/dx \qquad (1.2)$$

The kinetic theory of gases predicts that the rate at which the reactants and products diffuse across the imaginary boundary layer vary with temperature and pressure.

- Directly proportional to the temperature ($T^{3/2}$)

- Inversely proportional to the total system pressure ($1/P_T$)

For gaseous reactions, as the diffusion rate (D) varies inversely with pressure, gas mass-transfer rates can be enhanced by reducing the pressure in the reactor. This is advantageous for Low Pressure Chemical Vapor Deposition (LPCVD) systems, which are extensively employed in semiconductor processing.

In a LPCVD reactor (~1 torr) the diffusivity of the gas species is increased by a factor of 1000 over that of atmospheric pressure and this is only partially offset by the fact that the boundary layer (the distance across which the reactants must diffuse) increases by less than the square root of the pressure .

1.4.3 Rate Limiting Steps

The rate limiting step of a CVD reaction is critical since it will help to optimize the deposition reaction, obtain the fastest growth rate and, to some degree, control the nature of the deposit [6].

The rate limiting step can be either determined by :

a) Surface reaction kinetics

b) Mass transport

c) Gas-phase kinetics (a more uncommon occurrence)

The rate of deposition can be controlled by a reaction at or near the surface or by mass transport in the gas. Mass transport involves moving the gas to the surface and removing the products away. If the process is controlled by the surface reaction, i.e. reaction rate is limited by the rate of surface reaction,

the deposition mechanism of the solid film follows the empirical Arrhenius behavior [7,8]:

$$G.R. = K \exp(-E_a/RT) \tag{1.2}$$

G.R. is the growth rate of the film (Å/min)

E_a is the activation energy of the chemical reaction

R is the gas constant

T is absolute temperature (K)

K is constant

According to this equation, the reaction rate increases with increasing temperature. There is a linear plot of log (Å/min) vs.1/T.

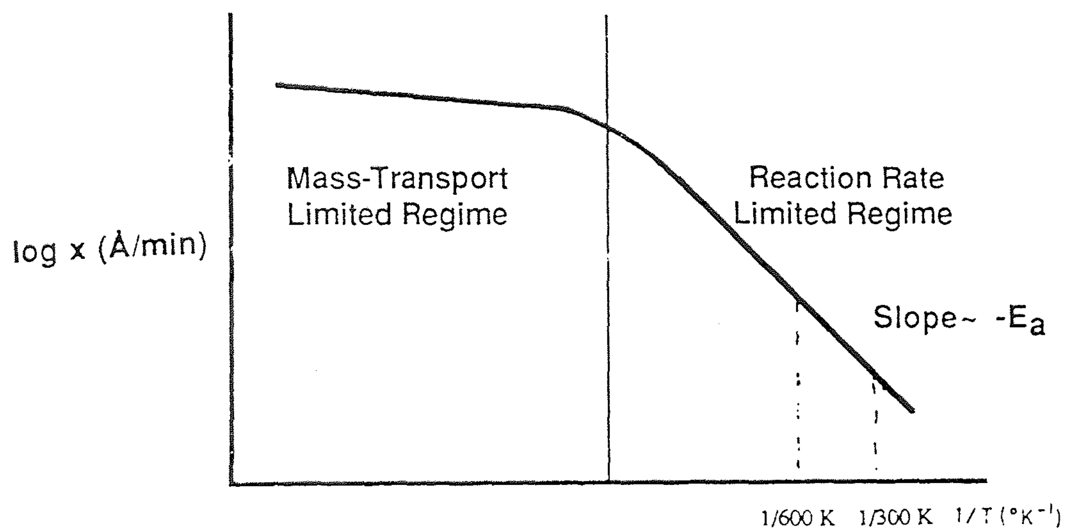

Figure 1.4 Temperature dependence of growth rate for CVD films

In the case of control by surface reaction kinetics, the rate is dependent on the amount of reactant gases available on the surface. At low temperatures

and pressures, the reaction occurs slowly step by step. Eventually the arrival rate of reactants exceeds the rate at which they are consumed by the surface reaction process. Under such conditions the deposition rate is *surface reaction rate limited.* This implies that uniform deposition rates throughout the reactor require conditions that maintain a constant reaction rate. The deposition rates can sometimes be changed by adding elements which can change the catalytic behavior of the substrate. At lower deposition rates, it is sometimes desirable to have surface kinetics control to obtain an even coating. Thus the rate at which the reactant species arrive at the surface is an important factor because their concentration does not limit the growth rate. As the surface reaction rate generally increases with the increase in surface concentration, non-uniform gas phase concentration produced by local depletion of reactants within the reactor can result in deposition non-uniformities. An example of such an effect is the depletion of the reactants from a gas by their deposition on wafers located at the inlet of an end-feed reactor tube. Wafers near the outlet end are consequently exposed to gases containing lower concentrations of reactants than those at the inlet end of the tube.

To obtain the highest rates of deposition, conditions should be selected to insure that kinetics controls the reaction. At high temperatures, the reaction rate exceeds the rate at which the reactant species arrive at the surface. In such cases, the reaction cannot proceed more rapidly than the rate at which reactant gases are supplied to the substrate. In this regime the temperature control is not very critical but the same concentration of reactants must be present in the bulk

gas regions, as the arrival rate is directly proportional to the concentration of the bulk gas. Thus, to insure films of uniform thickness across a wafer, reactors which are operated in the mass transport limited regime must be designed so that all the locations of the wafer in a run are supplied with an equal flux of reactant species. Thus, at high temperatures the deposition is usually controlled by mass-transport reaction rate, while at lower temperatures it is surface-reaction rate limited (Figure 1.4). In the actual process the temperature at which the deposition condition moves from one of these growth regimes to the other is dependent on the activation energy of the reaction, and gas flow conditions in the reactor. Adsorption of decomposition products or depletion of the reactants on the surface of the substrate may be an additional factor retarding the film growth [1].

1.4.4 Reactant Gas Concentration and Velocity

When a stream of gas is flowing in bulk past a solid wall, the gas adheres to the solid wall at the actual interface between solid and reactant gas. The adhesion may occur due to the force fields at the boundary, which are also responsible for the interfacial tension between solid and gas. If, therefore, the wall is at rest in the reference frame chosen for the gaseous - solid system, the velocity of the fluid at the interface is zero. Since at distances away from the solid the velocity is finite, there must be variations in velocity from point to point in the flowing stream. Therefore, the velocity at any point is a function of the space coordinates of that point, and a velocity field exists in the space occupied by the reactant gas.

The thickness of the boundary layer depends on the gas flow velocity and is given by equation 1.3:

$$\Delta = [x/Re]^{1/2} \qquad (1.3)$$

Δ - thickness of the boundary layer

x - distance from inlet in flow direction

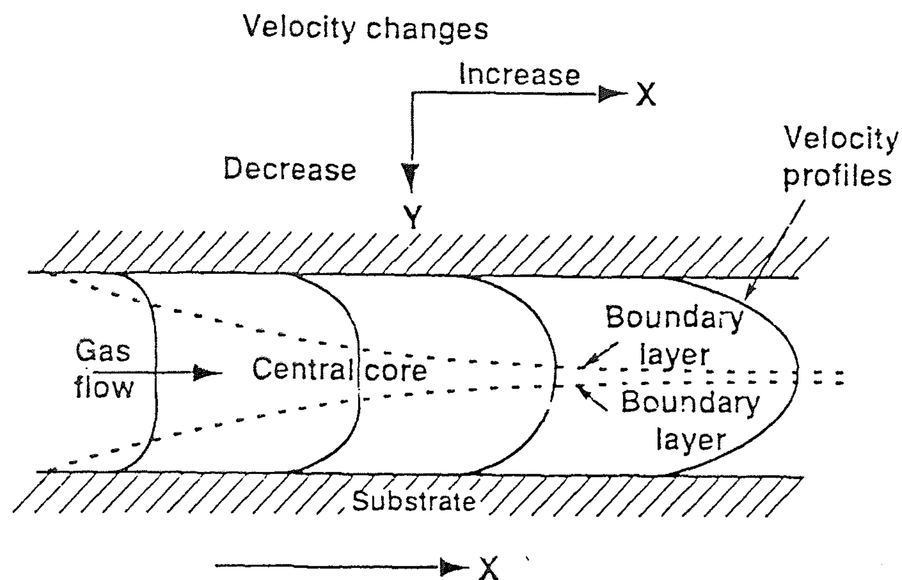

Figure 1.5 Changes in reactant velocity along a tubular reactor

Figure 1.5 shows a typical velocity pattern in a horizontal tube. As mentioned above, a steep velocity gradient is noticeable going from maximum velocity in the center of the tube to zero velocity at the surface of the wall. The Reynolds number is the flow velocity times the gas density divided by the gas viscosity times the reactor diameter. As the gas velocity increases, the Reynolds number will also increase and the thickness of the boundary layer will decrease gradually. As the gases flow down the tube they become gradually depleted. Due

to this the deposition will cease at some point downstream. At low velocities gases tend to flow without lateral mixing, and the adjacent layers slide past one another. There are neither cross-currents nor eddies. This regime is called the *laminar flow* where most of the CVD reactions are carried out. The reactant concentration is illustrated in the Figure 1.6 below.

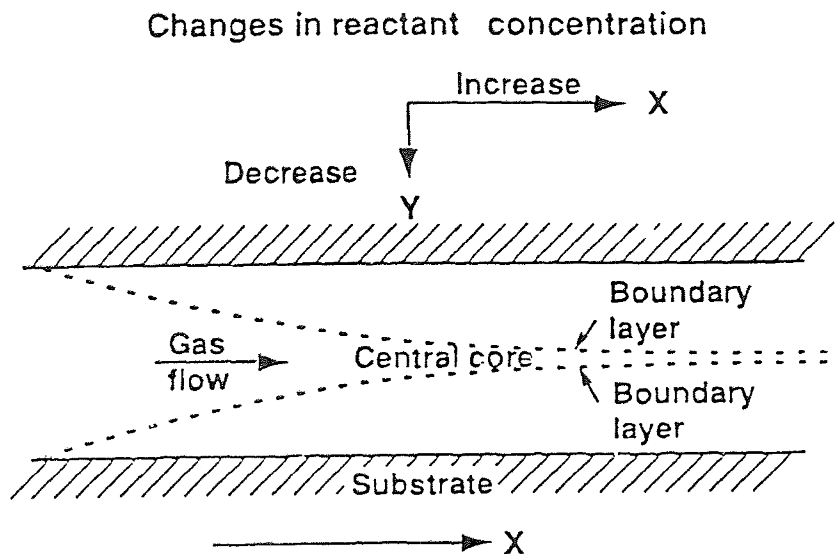

Figure 1.6 Changes in reactant concentration in a tubular reactor

1.5 Advantages of CVD

The reasons for the success of CVD are simple:[9]

- CVD is a relatively uncomplicated and flexible technology through which a great variety of chemical compositions can be deposited
- The deposition rate is high and thick coatings can be readily obtained. The process is generally competitive and, in many cases, more economical than the Physical Vapor Deposition (PVD) process.

CVD is an important method of synthesizing the films used in the fabrication of integrated circuits as well as other microelectronics devices

1.6 Limitations of CVD

Fundamental limitations of CVD are the chemical reaction feasibility and the reaction kinetics that govern the CVD process. Technological limitations of CVD include the unwanted and possibly deleterious but necessary by-products of reaction that must be eliminated, and the particle contamination generated by homogeneous gas phase nucleation that must be minimized.

1.7 Objectives of the Research Work

A study to investigate the incorporation of silicon into SiC, Si-C-N and Si_3N_4 films from various organosilanes has been carried out. The Arrhenius activation energy for the synthesis of silicon, silicon carbide and silicon nitride films from silane and various organosilanes have been summarized (165-210 kJ/mol). This value is found to be close to the energy required to remove hydrogen from a hydrogenated silicon surface. Recent works have indicated that this is the rate limiting step in the mechanism for the deposition of silicon from silane. It is proposed here that this hypothesis can be established for the synthesis of silicon carbide, silicon nitride and silicon carbonitride films. The gas phase chemistry, and the reaction geometry has been studied in order to understand the factor influencing the formation of silicon carbonitride films

The thesis has been split into five chapters. The second chapter will review the applications and properties of silicon carbide (SiC) along with a critical review of various chemical vapor deposition (CVD) techniques. The third chapter will be devoted to describing the experimental set-ups, description of LPCVD reactor, experimental parameter details and summary of characterization studies involved. The various theories about silicon carbide deposition are explained in the fourth chapter and the results about the nature of the silicon carbonitride film and the conclusion will be presented in the final chapter.

CHAPTER 2

LITERATURE REVIEW

Silicon carbide films prepared by chemical vapor deposition (CVD) remains of importance for both structural and electronic applications. Silicon carbide is a hard oxidation resistant material which has been used in both electronic and structural applications. A range of gaseous precursors has been used for the deposition process, under widely varying conditions of input gas compositions, temperatures and pressures. Group V element additions make SiC n-type semiconductors while group III elements make them p-type.

2.1 Preparation

Silicon carbide is a compound with a dissociation temperature of 2830°C. A phase diagram is shown in the figure 2.1. The deposition of silicon carbide will take place when the amount of C and Si introduced in the gases is greater than the equilibrium amounts in the corresponding precursors [10].

2.2 Properties

Currently, there is much interest in the preparation methods of hydrogenated amorphous silicon carbide. Besides, its chemical inertness, hardness and radiation resistance, the energy gap and thus its electronic and optical properties can be continuously changed by controlling the composition and the hydrogen

content. The thermal conductivity of SiC materials is seen to be significantly higher than that of conventional semiconductors.

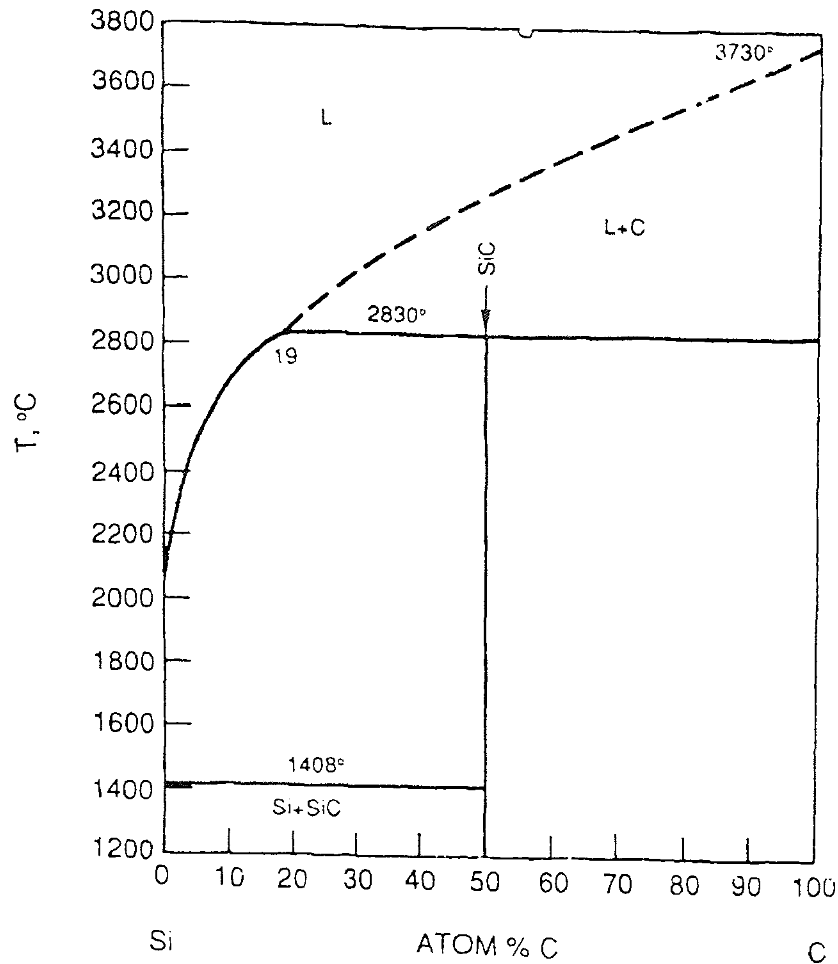

Figure 2.1 Phase diagram of the SiC system

Silicon carbide exhibits a dielectric strength of 10 times that of silicon and a thermal conductivity 5 times that of silicon. Amorphous SiC offers a unique combination of properties as reflected in its mechanical strength, chemical stability, high x-ray and optical transmission, and wide semiconductor bandgap [11,12]. These two properties combined with its general availability render it

ideally suited for use in high-power amplifiers, switches, and diodes. SiC is the only wide bandgap (WBG) material that has a viable native oxide (SiO_2), thereby rendering it useful in an enhancement/depletion transistor configuration [13]. There are two main structures of silicon carbide, a cubic form (β-SiC) and α-SiC which represents many different hexagonal polytypes. The beta silicon carbide is stable at lower temperatures and converts to the alpha form at about 2000°C. The wide energy bandgap of 2.2 e.v. for β-SiC and 3 e.v. for α-SiC makes silicon carbide useful as a high temperature semiconductor. P-N junction leakage in SiC is many orders of magnitude less than that in conventional semiconductors. Exploitation of this property has led to the demonstration of nonvolatile random access memory (RAM) and charge-coupled devices. Silicon carbide has also been of interest because of its optical, photoelectric, photoluminescence and electroluminescence properties.

Table 2.1 Properties of CVD SiC

Density (g/cm^3)	3.2
Thermal Conductivity (W/M.K.)	4.5
Strength (ksi)	100
Modulus (Msi)	60
Hardness (kg/mm^2)	61
Refractive Index	2.65

2.3 Applications

The properties of CVD SiC that are listed in Table 2.1 make possible a wide variety of applications. For structural applications, its erosion resistance and hardness makes SiC useful as an abrasion and an erosion resistant coating. The hot pressed and sintered materials have been considered for engine components. For example, attempts have been made to produce large engine blades from the hot pressed materials. Silicon carbide high-power devices will begin to replace silicon devices and vacuum tubes at frequencies up to 1 GHz. This replacement will be complete early in the next decade.

The development of a low pressure chemical vapor deposition (LPCVD) process for synthesizing good quality SiC films would open a wide range of applications including membrane materials for x-ray masks, radiation-hard and high-temperature devices, emitters for heterojunction bipolar transistors, and windows for solar cells. The purest form of silicon carbide, at least in the polycrystalline form, is the CVD material. The absence of significant amounts of impurities in the grain boundaries makes the material more oxidation and corrosion resistant than other forms. In addition, the CVD material is strong and has been used to form fibers and a CVI matrix in C/SiC and SiC/SiC composites. Yarns have also been coated with CVD SiC. Carbon yarn with a SiC coating is more oxidation resistant and will be wet by aluminum in an infiltration process for forming C/Al composites. Silicon carbide fibers on a tungsten substrate are being reexamined with appropriate coatings to make them useful in metal matrices. CVD SiC coatings have also been used to improve the erosion or moisture

resistance of materials. The addition of SiC on the surface of boron fiber has improved its high temperature properties. Tools bits, valves and optical fibers have been coated with SiC to improve the erosion and moisture resistance of the materials.

2.4 Methods of Thin Film Deposition

The structure of thin films, and their method of preparation also play a vital role in determining the film properties. Thin film fabrication is a complicated process which involves many controlled processing parameters. The time of processing, equipment cost, throughput and quality of films are important factors for a successful commercial production. Many techniques are available in the present technology for film fabrication. But, the most common methods that are used for economic production are Physical Vapor Deposition (PVD) and Chemical Vapor Deposition (CVD). The reason for choosing the CVD method for this study is also explained.

2.4.1 Physical Vapor Deposition

In this method, thin film material in gaseous form is allowed to deposit on the substrate directly. No chemical reaction is involved in this method. The sequence of steps for a PVD process proceed as follows:

1. The material to be deposited (solid or liquid source) is physically converted to a vapor phase.

2. The vapor is transported across a region of reduced pressure (from source to substrate).
3. The vapor condenses on the substrate to form a thin film.

Depending upon the method of converting the deposition material to vapor phase, PVD is classified as :-

1. By evaporation
2. By Glow discharges and plasmas
3. Sputtering
4. Ion Plating

2.4.2 Chemical Vapor Deposition

Chemical vapor deposition has several advantages over other methods of film deposition. These are listed below:

1. Unlike in PVD, there is no radiation like e-beam involved, therefore, there is no possibility of the damage of the film or the substrate by this method.
2. Since the whole area of the substrate is equally exposed to the reactant, good uniformity of film thickness is achieved.
3. Selective deposition of film onto the substrate can be done by masking unwanted portions of the substrate.
4. Chemical vapor deposition (CVD) offers an excellent opportunity of impurity doping in device fabrication. This is possible by simply mixing the dopant with the reactant.

5. Stoichiometric control of the film can be easily achieved by adjusting the process parameters like deposition temperature, pressure, and flow rate.
6. Low maintenance cost of the equipment makes it an attractive method for large scale production.

2.5 Types of CVD Processes

CVD processes can also be classified according to the type of energy supplied to initiate and sustain the reaction: (1) Thermally activated reactions at various pressure ranges, which comprise the vast majority of CVD processes; heat is applied by resistance heating, rf induction heating, or infrared heating techniques. (2) Plasma promoted reactions, where an rf (or dc)- induced glow discharge is the source for most of the energy that initiates and enhances the rate of the reaction. (3) Photon induced reactions, where a specific wavelength radiation triggers and sustains the reaction by direct photolysis or by an energy transfer agent, such as uv-activated mercury.

2.5.1 Thermally Activated CVD

This process uses direct thermal energy for the chemical reaction. The simplest type of this method is conventional atmospheric pressure CVD (APCVD) where, the reactant gases are introduced in the reactor at normal atmospheric pressure [14,15]. Energy is supplied by resistance heating, by rf induction techniques, or by infrared radiation to heat the substrate to an appropriate temperature. Since the APCVD processes are generally conducted in the mass-transport limited

regime, the reactant flux to all parts of every substrate in the reactor must be precisely controlled. This places constraints on the reactor geometry and gas flow patterns. The advantage of APCVD is its simplicity, no vacuum pumps are needed. The disadvantage is the tendency for homogenous gas phase nucleation that leads to particle contamination, unless special optimized gas injection techniques are used. Currently, APCVD is used only for low temperature oxide (LTO) deposition and epitaxy.

Lowering the gas pressure will primarily enhance the mass flux of gaseous reactants and products through the boundary layer between the laminar gas streams and substrates. Also the mass flux (Ji) of the gaseous specie is directly proportional to D/δ and is given by

$$Ji = -D(P_i - P_{io})/\delta RT \tag{2.1}$$

δ - thickness of the boundary layer

P_i- vapor pressure in bulk phase

P_{io} - vapor pressure at surface

In a LPCVD reactor, the diffusivity of the gas species is increased by a factor of 1000 over that of atmospheric pressure. This is only partially offset by the fact that the boundary layer (the distance across which the reactants should diffuse) increases by less than the square of the pressure. The net effect is that there is more than an order of magnitude increase in the transport of reactants to (and by-products away from) the substrate surface. The increased mean free

path of the gas molecules means that substrate wafers can be stacked closer together, resulting in higher throughputs. Hot-wall systems use the reaction energy by a method that heats the wafers, the wafer holder, and the chamber walls. Low pressure CVD is widely used in the extremely cost competitive semiconductor industry for depositing films of insulators, amorphous and polycrystalline silicon. Epitaxial growth of silicon at reduced pressure minimizes autodoping (contaminant of the substrate by its dopant), a major problem in atmospheric pressure epitaxy. This is a suitable method for SiC deposition.

2.5.2 Plasma Enhanced Chemical Vapor Deposition (PECVD)

Plasma deposition [16-20] is a combination of a glow discharge process and low pressure chemical vapor deposition. Plasma Enhanced CVD uses an rf induced glow discharge to transfer energy into the reactant gases, allowing the substrate to remain at a lower temperature than in LPCVD processes. Glow discharges are usually created at low pressures in the 0.01 to 1 torr range. This causes breakdown of molecules into reactive species like ions, electrons, etc. An electric field due to a.c., d.c. or microwave sources across two electrodes creates plasma region between two electrodes. The molecules can be near to the ambient temperature but the breakdown electrons will be at a higher temperature causing the reaction. Thus, this method can be employed at a relatively low temperature and it is useful for temperature sensitive material. Lower substrate temperature also provides a method of depositing films on substrates that do not have the thermal stability to accept coating by other methods (the most important

being the formation of silicon nitride and SiO_2 over metals). In addition, PECVD can enhance the deposition rate when compared to thermal reactions alone, and produce films of unique compositions.

The major limitation of PECVD is that the deposition of pure material is virtually impossible. Because of the reduced substrate temperature, desorption of product gases is ineffective resulting incorporation of these elements. Also the complexity of reactions make the synthesis of stoichiometric composition difficult.

2.5.3 Photon-Induced Chemical Vapor Deposition (PHCVD)

Photon-Induced chemical vapor deposition uses high energy, high intensity photons to either heat the deposition substrate, or to dissociate and excite reactant species in the gas phase. This technique enables deposition at extremely low (i.e.room) substrate temperatures. In the case of substrate surface heating, the reactant gases are transparent to the photons, and the potential for gas phase reaction is completely eliminated. In the case of reactant gas excitation, the energy of the photon can be chosen for efficient transfer of energy to either the reactant molecules themselves, or to a catalytic intermediary, such as mercury vapor. PHCVD films show good step coverage, but may suffer from low density and molecular contamination as a result of the low deposition temperature. Depending on the energy source there are 2 classes of PHCVD reactors: a) UV Lamp and b) Laser PHCVD reactors.

UV lamp reactors generally use mercury vapor for energy transfer between photons and the reactant gases. UV radiation at 253.7 nm wavelength

is efficiently absorbed by mercury atoms, which then transfer energy to the reactant species. The advantage of this method is low deposition temperature needed for films like SiO_2 and absence of radiation damage. The limitation is that the deposition rates are typically slower than in other low temperature techniques [21].

Laser PHCVD reactors [22] offer the advantage of frequency tunability and high intensity light source. The energy from the high intensity laser also increases the reaction rate. Laser PHCVD also opens the possibility of CVD writing (i.e. patterned deposition by spatial control of laser).

2.6 Summary

The common methods of film deposition techniques by chemical vapor deposition (CVD) were described. The advantages of CVD over PVD were also described. The low pressure chemical vapor deposition (LPCVD) was found to be a superior method compared to atmospheric pressure chemical vapor deposition (APCVD). Therefore, in this study, hot wall low pressure chemical vapor deposition system was employed.

CHAPTER 3

EXPERIMENTAL PROCEDURE

3.1 LPCVD Reactor

The low pressure chemical vapor deposition reactor is schematically shown in Figure 3.1. The horizontal reaction chamber consists of a 11.5 cm diameter fused quartz tube, 178 cm long, encapsulated with a three-zone, Lindberg heating furnace. The heating furnace used Lindbar silicon carbon heating elements which could raise the temperature of the reaction chamber up to 1200°C. The entire tube was insulated from the environment by a ceramic enclosure. A varying temperature profile could be set within the three zones, even though this facility was rarely used. Temperature control and stability was achieved by the associated electronic feedback circuits, which included calibrated K type thermocouples, that sensed the temperature of the reaction zone. The temperature inside the furnace was measured relative to a calibrated type K thermocouple.

The pressure inside the chamber was monitored at the input end of the furnace by an MKS baratron gauge with a range of 10 torr. The other end of the reaction chamber was connected to a vacuum station comprised of a booster pump and a mechanical backing pump. The booster pump was used to enhance the flow of gases and thereby pumping speed. The mechanical backing pump did the real pumping and this combination provided a vacuum as low as 5 milli torr. Nitrogen ballast gas was used in the booster pump to dilute any hazardous

outgoing gas. Apart from this, an oil filter system was used to filter micron sized particles from oil and thereby increasing the lifetime of the pump.

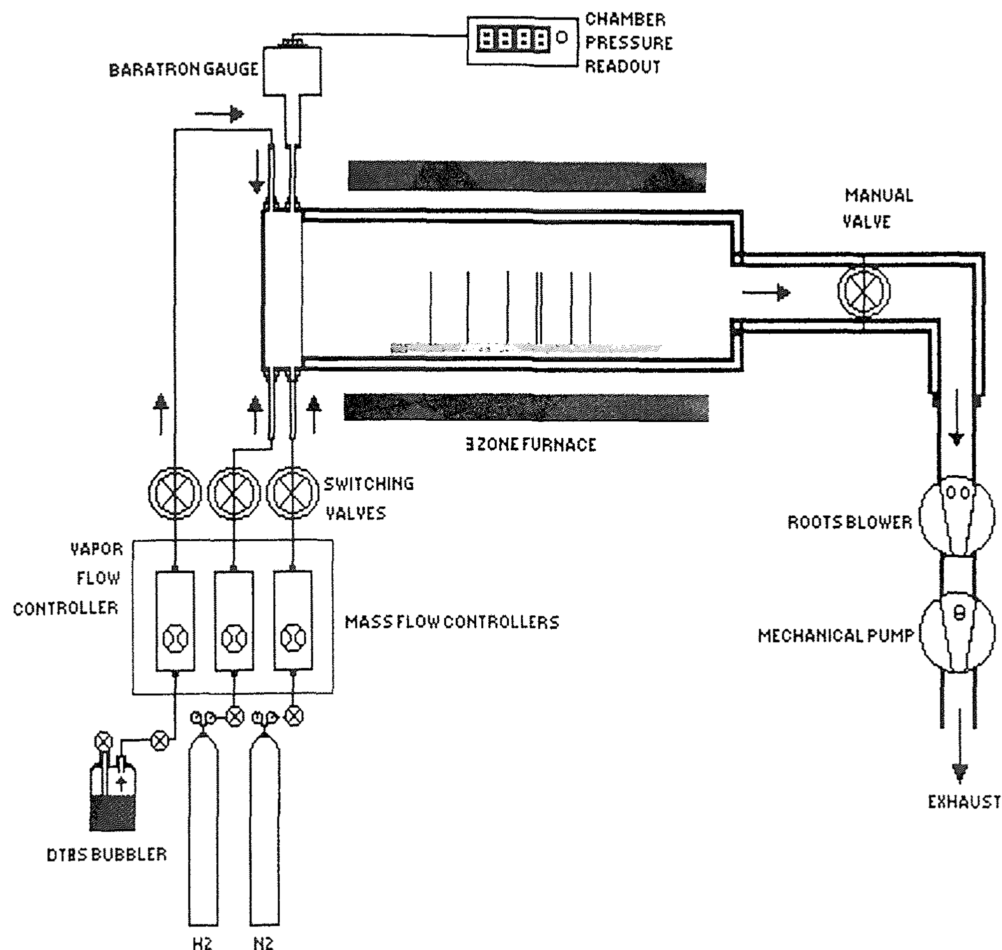

Figure 3.1 Schematic representation of the LPCVD reactor

The reaction chamber was sealed on both ends by end caps and metallic lids. During the heating process, thermal expansion of O-rings may cause leakage of outside air in to the system. To avoid this problem, end caps designed for this reactor have a provision for cold water circulation (not shown in

the figure 3.1) to prevent overheating of the O-rings. A manual valve at the output end was used to control the removal rate of gases and thereby maintaining a steady pressure inside the chamber. The precursor was delivered inside the chamber, in a controlled manner using mass flow controllers. The calibration of these flow controllers is described in a later section. A spare nitrogen mass flow controller was installed to incorporate any necessary additional reactant gas into the chamber or for backfilling. This spare controller could be calibrated for the gases other than nitrogen [23].

3.2 Pre-Deposition Procedure

3.2.1 Leak Check

An air leak into the chamber may arise due to improper delivery line connections and improper chamber end cap connections. Such leakage will affect the quality of deposits, therefore, routine leak checks were conducted keeping all valves and mass flow controllers fully open. After evacuating the chamber, the manual valve was closed and from the pressure rise in the reactor the leak rate was calculated. Typical leak rates were of the order of 0.2 -0.5 sccm. This was mostly due to outgassing from the deposits on the chamber wall resulting from the previous depositions.

3.2.2 Flow Rate Calibration

Generally the flow rate of the precursor is expressed in units of sccm, i.e., standard cubic centimeters per minute. This is the volume that would be

occupied by the precursor, which is measured at standard temperature and pressure, as a result of flow for one minute. Inorder to verify the rate of flow, the precursor was delivered into the CVD reaction chamber at a known initial pressure and at room temperature, using the standard flow controller which was set to control at the desired flow. The manual output valve was then closed and the rise in chamber pressure over a fixed time interval was measured. Assuming that the temperature inside the reaction chamber was at T_r (i.e., room temperature) and the precursor to be an ideal gas under these conditions. The Ideal Gas Law can be applied,

$$PV = nRT \tag{3.1}$$

Since the chamber volume, V, is fixed, and was determined by the geometrical measurements and using a previously calibrated N_2 flow meter,

$$\frac{\partial n}{\partial t} = \frac{V}{R * T_r} * \frac{\partial P}{\partial t} \tag{3.2}$$

where, t is the time.

At the standard condition of temperature (273 K) and pressure (760 torr) therefore,

$$V_s = \frac{nRT}{P} = nR * \frac{273}{760} \tag{3.4}$$

and,

$$\frac{\partial V_s}{\partial t} = R * \frac{273}{760} * \frac{\partial n}{\partial t} \tag{3.5}$$

Substituting equation (3.3) into (3.5), gives the flow rate at room temperature, T_r,

$$F.R. = \frac{\partial V_s}{\partial t} = \frac{V}{760} * \frac{273}{T_r} * \frac{\partial P}{\partial t} \tag{3.6}$$

Where, V is the volume of the reaction chamber (which was measured as 18,530 cm^{-3}), and $\Delta P/\Delta t$ is the rate of increase in pressure. Equation 3.6 was used to calibrate the flow rate of the reactants.

3.3 Deposition Procedure

3.3.1 Wafer Loading

Films were synthesized on virgin silicon substrates. The specification of silicon wafers are depicted in Table 3.1. These substrates were first labeled and weighed, using an electronic weighing balance with an accuracy of 0.01 mg. Then, they were mounted vertically on a fused silica boat with 12 single wafer slots and 10 double wafer slots. Single and double wafer slots alternated along the length of the boat with a distance of 1.25 cm between them. Dummy wafers were placed at the first two slots and the last two slots in each run. For convenient handling of the boat, the first dummy wafer was mounted on the second single wafer slot at 6 cm from the front end of the boat. The virgin wafers were placed on subsequent slots. Some wafers need to be deposited on one

side only, in order to measure the stress of the film. This was accomplished by placing two wafers together, back to back, on a double wafer slot. The quartz boat was then placed with its front at 65 cm downstream, ensuring that they were placed in the middle zone of the furnace. The front end of the chamber was then closed and the chamber was pumped down.

3.3.2 Film Deposition

The reaction chamber and the reactant delivery lines were evacuated for about 30 minutes. Silicon carbonitride thin films with varying composition and properties can be synthesized in a LPCVD reactor by adjusting various deposition parameters including temperature, pressure, gas composition and time of deposition. The wafers were initially loaded in the reaction chamber and the outlet valve was opened to remove the air from the chamber and create a vacuum. Water circulation and fans were used to cool the end cap O-rings. The booster pump was turned on to generate high vacuum inside the chamber. The reaction chamber was then gradually heated to the deposition temperature and stabilized for fifteen minutes to ensure thermal equilibrium. The temperature was initially raised to 250°C and then increased gradually in steps of 150°C until it reaches the deposition temperature. Once thermal equilibrium was reached, the reactant was allowed to flow for a stipulated time. The valve for the precursor TDMAS was then opened and the gas was passed at constant flow rate in the reaction chamber. The outlet valve was then closed so as to adjust the operating

pressure at which the experimental run is to be carried out. The experiment was carried out for three hours.

After the deposition, the furnace was left to cool at its normal rate. The chamber was opened the next day, by breaking the vacuum. This was done by delivering a fixed flow of nitrogen in to the chamber, when the output valve was completely closed. This would bring the chamber to atmospheric pressure and thereby enabling the front lid to open. The experiments yielded a variety of films which were carefully subjected to physical and chemical analysis. These characterization procedures were aimed at standardizing the processing conditions to produce films that are suitable for making a X-ray mask membrane. Fourier transform infrared (FTIR) analyses were done on the synthesized films to

Table 3.1 Specifications of the Si wafer

Source	Silicon Sense Inc.
Diameter	100 mm
Orientation	<100>
Thickness	525 ± 25 µm
Type/Dopant	p/Boron
	n/Phosphorus
Resistivity	5 - 15 Ω-cm
Grade	Test

examine the vibrational modes of the deposited films. Stress on the films was measured and calculated by the principle of radius of curvature difference. Refractive index and thickness of the films were measured by ellipsometry and interferometry respectively. The elemental composition analyses were done by

Auger electron spectroscopy (AES) and X-ray photoelectron spectroscopy (XPS). X-ray diffraction analyses were performed in order to verify the amorphous or crystalline nature of the deposits. Mechanical properties such as Young's Modulus and hardness of these films were measured using a Nano Indenter.

3.4 Film Characterization Techniques

3.4.1 Initial Analysis

Once the wafers were taken out of the reactor, they were weighed again. The difference in weights before and after the reaction would give the mass of the film deposited. The mass divided by the time of deposition would give the *growth rate*.

Film thickness was measured by a Nanospec Interferometer which bases its estimates on the monochromatic light interface fringes formed within a zone limited by the sample surface and a semi-transparent mirror. The surface of the wafer to be measured was flat with respect to the objective lens of the microscope. It was ensured that the surface of the film was focused properly for accurate results. The measuring spot consists of a very small hole made in a metal mirror located in the black cell bolted to the underside of the spectrophotometer. The film type was entered by depressing the proper numeral on the numerical display panel and then pushing "ENTER". The printer will immediately print out the film type selected. There was a option to enter the refractive index. The refractive index was entered and the computer calculated

the thickness accordingly. The thickness of the film deposited on one side was measured at five different points on the wafer i.e. 1 cm from the edges of both the equatorial and the longitudinal axis, and at the center, see Figure 3.2. Uniformity in radial distribution of the deposits was then estimated from the relationship: $(T_{max} - T_{min})/(T_{max} + T_{min})*100$ where, T= the average film thickness.

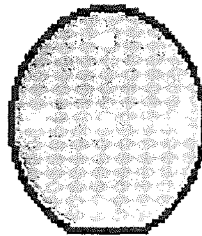

Figure 3.2 Schematic diagram of a typical silicon wafer showing points where thickness was measured

3.4.2 Refractive Index Measurements

Refractive index of the film was determined using an Rudolph Research AutoEL ellipsometer. The measurement technique is mainly concerned with the measurement of changes and the state of polarization of light upon reflection with the surface. It employs monochromatic, plane polarized light with its plane of polarization 45° to the plane of incidence. When the elliptically polarized light is reflected from an absorbing substrate its state of polarization is changed. The ellipticity of the reflected beam is determined by the relative phase difference δ and azimuth ψ. An in-built computer program numerically solves the equations

generated by these δ and ψ and the refractive index and the thickness of the film is obtained.

The AutoEL power was turned on and wait fifteen minutes for warm-up. The Rudolph check sample was placed on the sample stage and press CONTINUE. The sample was positioned so that the rectangular area is under the measurement of the light beam. The sample height was adjusted to reflect the light beam into the analyzer entrance aperture. The screws were rotated until a white spot was visible at the center of the reticle. Once the initialization was complete, run program 20 to measure the refractive index. The approximate value of the thickness was entered. This procedure was repeated by rotating the silicon wafer so as to obtain the average refractive index. Similarly, place the new sample on stage and follow the same procedure to determine the refractive index of other samples. The index of refraction is an important parameter which gives indication of stoichiometry of the film. This parameter is also used in measuring thickness using interferometry. Measurements were taken in the range of 500-2900 nm.

3.4.3 Infra Red Spectroscopy

Infra red spectroscopy is a powerful method by which one can detect the presence of particular type of molecular vibration. Some materials will absorb certain frequencies in the infra-red region (wavelengths 2 to 25 microns) because of the excitation of vibrational energy transitions in molecular species. In the same way the electronic transitions in atoms can absorb radiation of

specific frequencies, the vibration of a molecule (stretching or bending) will have a resonance value, and it will be excited by any radiation of this frequency. When IR radiation of a particular frequency impinges a sample containing molecular species, it may or it may not be absorbed. If all frequencies are passed through, some will be absorbed to varying degrees depending on the molecular species involved. The intensity of the return radiation therefore depends upon the vibrational mode of the molecules. The presence of a particular molecular vibration can be detected by an absorption or transmission peak in the spectrum.

The power supply was turned on. A supply of desiccant was placed within the system that removes any water vapor or carbon dioxide present. Place the reference wafer vertically in such a manner that the polished surface faces the laser beam. The background spectra was obtained with 256 scans for accurate results. The purpose of running the test on the reference wafer is that it will show the peaks and characterization without any deposition. Now, place the wafers that were subject to the chemical vapor deposition of the film. The spectra of the film was obtained for 256 scans. Infrared spectroscopic analysis was done on a routine basis using a Perkin Elmer 1600 series FTIR spectrophotometer and Perkin Elmer 580 spectrophotometer to determine the bonding characteristics of the deposits.

3.4.4 Stress Measurements

Stress develops in the film due to the difference in the thermal coefficient of expansion of the film and the substrate, and also due to defects developed

during the growth process. Film stress was determined with a home-built system that measured changes in the radius of curvature of a wafer resulting from deposition on a single side.

Stress (σ_s) of the film is calculated using Stony's formula

$$\sigma_s = ED^2/6(1-\nu)Rt \qquad (3.7)$$

where E and ν are Young's modulus and Poisson ratio of the substrate. D, t are the substrate and film thickness' respectively and R is the radius of curvature of the composite. By convention R is negative for a convex wafer surface (compressive film stress) and positive for a concave wafer surface (tensile film stress).

The deposition for stress measurement films was achieved by placing the two wafers back to back. This wafer was then placed under the mirror on a circular shaped base. The power supply was turned on and the laser was also turned on. The distance between two points generated by light from two fixed and parallel He-Ne lasers was determined after reflection from the surface of a wafer before and after deposition. An angled mirror was used to project the reflection of the two points onto a wall where their separation could be more accurately measured. In the present set of experiments for the wafers used and considering the geometry of the instrument used, the equation reduces to

$$\sigma_s(\mathrm{MPa}) = 12.3R'/t\ (\mu\mathrm{m}) \qquad (3.8)$$

where R' is the difference of the deflection of the projected laser spots after and before deposition.

3.4.5 X-ray Diffraction Studies

X-ray diffraction techniques can be used to identify the phases present in samples from raw starting materials to finished product and to provide information on the physical state of the sample, such as grain size, texture and crystal perfection. Most X-ray diffraction techniques are rapid and non-destructive. X-rays are a portion of the electromagnetic spectrum having wavelengths from 10^{-10} to 10^{-8} m, although only 0.3 to 2.5 Å is used for x-ray diffraction. The X-ray source uses a high-energy (30kV) electron beam directed into a cooled metal target. As the electrons are decelerated in the target, several events produce x-radiation. Most of the electron beam energy is lost in collisions that set the atoms in motion and produce heat, which must be dissipated through the cooling water. Some electron energy is caught in the electric fields of the atom as the electrons decelerate and is reradiated as x-rays [24].

A small but significant portion of the electron beam collides with the electrons of the target atoms. Some target electrons are knocked out of their orbitals, leaving the target atoms in a high-energy excited state. The energy stored is brief, and the stored energy is released as the electrons from other orbitals drop into the vacant orbital. These electron transitions are of distinct energy jumps, and the radiation emitted has specific wavelengths. Thus, x-rays exiting the target have a few strong characteristic concentrations of specific

wavelengths superimposed on the white radiation. The characteristic spectrum of the x-ray is simple and few wavelengths have strong peaks.

Copper is typically used as the target because the Kα characteristic radiation is a useful wavelength, 1.5406 Å, and the target is easily cooled for high efficiency. The cooling system was turned on initially. A 2 mm $\times$ 2mm sample was placed in the X-Ray machine. Then the power for the main system was turned on. The power for the X-ray system was turned on and the system was allowed to cool for about 5 minutes. The X-ray machine was switched on which was indicated by the appearance of a red light. The voltage rose as it was preset to 10 kV. This is because the voltage is the driving force for the current { $I = V/R$ }. The voltage was slowly increased by 4 units and the current was raised by 2 units. It was kept increasing in this manner until the voltage reaches to 30 kV volts and the current to 20mA. Now X-ray diffraction patterns were studied to find the structure of the deposited films using an IBM PC based Rigaku diffractometer with a Cu target.

3.4.6 Compositional Analysis

The elemental composition and chemical states were studied by X-ray photoelectron spectroscopy (XPS) and Auger electron spectroscopy (AES) using a Perkin-Elmer 570 ESCA/SAM. The initial event is the ejection of an electron from one of the core electronic levels by an incident x-ray photon. The kinetic energy (KE) of the photoemitted core electron is:

$$KE = h\nu - BE + \Phi \tag{3.9}$$

where $h\nu$ is the energy of the exciting radiation. BE is the binding energy of the emitted electron in the solid, and Φ is the spectrometer work function.

Once the core hole is produced it is filled by an outer electron. When the electronic transition occurs energy is conserved by the emission of secondary electrons or by the emission of a photon. The Auger electrons or the photons emitted have relatively low kinetic energies ranging from approximately 50 to 2000 e.v. These low velocity electrons have a high probability of undergoing an inelastic collision with an atom in the matrix if they travel very far before leaving the surface. Only those electrons originating from the surface or a few atomic layers below the surface will contribute to an XPS peak. One of the most important capabilities of XPS is its ability to measure shifts in the binding energy of core electrons resulting from a change in the chemical environment. Hence the x-ray photoelectron spectroscopy is also known as electron spectroscopy for chemical analysis (ESCA). XPS is used for the chemical state identification of surface species and in-depth composition profiles of elemental distribution in thin films. It is also used for the compositional analysis of samples when destructive effects of electron beam techniques must be avoided.

Estimated Analysis Time:

- Requires a overnight vacuum pumpdown before analysis.
- Qualitative analysis can be performed in 5 to 10 min.
- Quantitative analysis requires 1h to several hours, depending on information desired.

Unmonochromatized Al Kα x-rays (1486.6 e.v., 25W) were the X-ray photoelectron spectroscopy (XPS) excitation source; a 5kV, 1μA electron beam was rastered over a square 250 μm on a side during Auger analysis. The base pressure of the system during analysis was 2 X 10^{-9} torr. Auger depth profiles were generated using a 4 kV, 3 μA Ar ion beam rastered over a 5 X 8 mm area. The core level binding energies were referenced to the Au $4f_{7/2}$ line at 83.9 e.v. A low energy electron foiled gun was also used for charging neutralization. Atomic compositions were calculated from XPS peak areas using the Perkin Elmer software cross-sectional values.

The limitations of X-ray photoelectron spectroscopy are [25]:

- Data collection is slow compared with other surface analysis techniques, but analysis time can be decreased substantially when high resolution or chemical state identification is not needed.
- Poor lateral resolution.
- Surface sensitivity comparable to other surface analysis techniques.
- Charging effects may be a problem with insulating samples. Some instruments are equipped with charge-compensation devices.
- The accuracy of quantitative analysis is limited.

3.4.7 Hardness and Young's Modulus Measurements

The hardness and Young's modulus of the Si-C-N films were determined using a Nano Instruments indenter. The system consists of a diamond tip, with the same area-to-depth ratio as the traditional Vickers pyramid, mounted on a loading

column that is suspended on thin leaf springs. At the top of the loading column is a coil and magnet assembly that provides a controlled loading force with a resolution of about 0.5 μN. The position of the indenter is determined by a capacitance displacement gauge which allows one to detect displacement changes of 0.2-0.3 nm. In this work, the maximum drift rate prior to testing was 0.1 nm/s, the loading rate was 200 μN/s to a maximum load of 4.5 mN, the hold time was 1 min., and the ambient temperature was kept constant with 1° at 21 $^{\circ}$C. In all cases a minimum of 16 indents were performed on each sample.

From the load displacement curve, the deformation contact depth (h_p) and elastic recovery depth (h_e) of the Si-C-N film can be measured. A linear least squares fit of the upper segment of the load displacment curve extrapolated to 0 yields the value of h_p. The difference between the maximum displacement and h_p yields the value of h_e. The hardness is obtained at the maximum displacement using the formula :

$$H = P/A \tag{3.10}$$

where P is the applied load and A is the contact area calculated from the known geometry of the indenter

$$A = 24.56\, h_p^{2} + 225.94\, h_p^{3/2} + 519.61 h_p \tag{3.11}$$

Assuming that the area in contact remains constant during initial unloading and adopting Sneddon's solution for the elastic deformation of an isotropic elastic material, the elastic modulus is obtained from the contact stiffness S, the slope of the unloading curve, given by

$$S = dP/dh = 2\,E_r \qquad (3.12)$$

where h is the displacement of the indenter, and E_r is the composite modulus for the indenter/sample combination

$$E_r = [(1 - \nu^2_f)/E_f + (1 - \nu^2_i)/E_i)]^{-1} \qquad (3.13)$$

where E_f and E_i are Young's moduli for film and indenter, respectively, and ν_f and ν_i are Poisson's ratios for the film and the indenter, respectively. Since ν appears as a quadratic term and therefore represents only a small correction, we took ν_f = 0.3, while the values for the diamond indenter E_i and ν_i were taken to be 1010 GPa and 0.213, respectively.

The system used to apply the load to the indenter consists of a magnet and coil in the indentation head and a high precision current source. The relative height of the indenter and the sample should be high enough to make sure to avoid accidentally hitting the indenter when positioning the specimen holder on the table. The indenter was lowered slowly towards the surface at a constant rate of about 15 nm per second to avoid significant impact effect when it arrives at

the surface. It is necessary that the specimen must be thermally equilibrated with the Nanoindenter prior to the initiation of indentation. Once the sample was loaded, we ran the Nano Indenter software and it is fully menu-driven.

CHAPTER 4

LITERATURE REVIEW OF SILICON CARBIDE DEPOSITION

This study investigates the low pressure chemical vapor deposition (LPCVD) process for silicon carbide thin films synthesized from single organosilane precursors. Recent studies [26,27,28] have investigated the growth kinetics of the SiC films as a function of the processing parameters over the deposition temperature range of 650-900°C and total pressure in the range of 0.1 to 0.5 torr from diethylsilane (DES), di-t-butylsilane (DTBS), and methylsilane(MES). Grow et. al. proposed, based on LPCVD experiments, that the growth rate is observed to vary linearly with flow rate and pressure for DES [26], while for DTBS [27], a square root dependency is observed for deposition temperatures below 700°C yielding apparent activation energies of 165 and 105 kJ/mol for DES and DTBS.

The work of Johnson et. al. [28] indicated that an Arrhenius type behavior was observed at temperatures below 900°C yielding an apparent activation energy of 222 kJ/mol for methylsilane (MES). This indicates that Arrhenius behavior is observed in the temperature range from 650-800°C for different organosilanes with an activation energy varying from 165-210 kJ/mol. Thus there is a possibility that the deposition mechanism of silicon may have some similarities independent of what type of film is produced. Recent studies [26,27] have shown that at deposition temperatures above 700°C; a change in the slope for the Arrhenius plot occurred for DES, DTBS and TDMAS which indicates that there is a change in the deposition mechanism. Eversteyn [29] reported that

similar behavior has been observed for LPCVD silicon films deposited from silane. However, the cause of the change in slope for the deposition of silicon carbide is unclear.

Usually, the silicon to carbon ratio and the degree of the crystal structure present, varies as a function of temperature. The deposition mechanism also depends on the nature of the carbon and the silicon deposit; whether they are deposited individually or in groups.

4.1 Structure Study

The complex sequence of atomic migration events occurring on the substrates leads to observable nucleation and growth processes, resulting in the formation of actual film and coating structural morphologies that develop during chemical vapor deposition [11]. Vapor supersaturation and substrate temperatures are the two most important variables affecting growth morphologies. Vapor supersaturation indicates the film nucleation rate, whereas the substrate temperature affects the growth rate.

Initially the hydrogenated silicon and carbon molecules get adsorbed on the Si wafer; the molecules are surface diffused randomly and may have a greater opportunity to desorb because they are less firmly bound to the substrate. As the adsorbed molecules diffuse on the surface, they may encounter other diffusing molecules and form a pair. This molecule pair would be more stable than an isolated molecule and would be less likely to desorb. As the pairs diffuse on the surface, they may join other molecules, forming a larger and

stable cluster, until the cluster has a lower probability of desorbing, and a critical cluster or stable nucleus may be formed. Because the probability of diffusing molecules encountering each other depends strongly on the adsorbed molecules on the surface, it is a strong function of the arrival rate of the gases and the desorption rate of the by-products. After stable deposited nuclei formed, additional adsorbed molecules diffusing on the surface can either initiate additional nuclei or join existing nuclei. When the existing nuclei are close enough together, additional molecules are more likely to join an existing nucleus, and the number of nuclei saturated remains constant as the size of each nuclei grows. The saturation number of nuclei depends on the substrate, arrival rate of molecules, and the temperature. Thus, a continuous film is formed as the nuclei impinge on each other. Even after a continuous film is formed, the structure is strongly influenced by the thermal energy available for surface migration.

At very low temperatures, the adsorbed SiC molecules have little thermal energy and cannot diffuse significantly on the substrate surface before they are covered by subsequently arriving molecules. Once they are covered their random arrangement is locked into place, and an amorphous structure is formed. At higher temperatures, adequate surface diffusion is possible to allow a crystalline structure to form [30]. Thus there is a possibility that the mobility of the adatoms governs the amorphous to crystalline phase transition [31]. When incident atoms stick to the site at which they impinge on the substrate, an amorphous film is most probable, whereas increased mobility raises the probability of crystallization. Ohring [11] concluded that single-crystal growth is

favored by low gas supersaturation and high substrate temperatures, whereas amorphous film formation is favored by high gas supersaturation and low substrate temperature.

4.2 Role of Hydrogen During Deposition

Recent works [32-35] have demonstrated that the hydrogen surface coverage controls the deposition process under conditions of very low pressure and low temperature (< 600°C). For silane, an Arrhenius type behavior was observed for deposition temperatures below 550°C yielding an apparent activation energy of 193 kJ/mol. A plot of log (growth) rate vs the inverse temperature results in a linear graph up to around 550°C, followed by a region with a much reduced growth rate. It has been observed that the amount of surface hydrogen deposited during growth, decreased with the increase in the deposition temperature. This will result in the desorption of hydrogen at higher temperatures. A change in the reaction mechanism was observed as the temperature is increased. The activation energy has been observed to change clearly from 193 kJ/mole to around 25 kJ/mol. At higher deposition temperatures, the surface is almost free of hydrogen and sufficient number of surface sites are available for silane adsorption. The film growth is limited by the arrival and reaction rate of silane and the silicon adsorption rate becomes a rate controlling step. The activation energy is found to be very low in this range and the silane reaction order would be very close to one. The silicon adsorption at higher growth temperatures is counteracting the hydrogen desorption resulting in a net

non zero SiH surface coverage. There is a possibility that the growth may be influenced by the silane equilibrium pressure. At lower temperatures, the process may be controlled by the rate of hydrogen desorption from two surface SiH species which require an activation energy of around 188-210 kJ/mole. In this range the film growth would be limited by hydrogen desorption and the reaction order for silane is close to zero. Gates et. al. [32,33,35] observed at higher temperatures, that the hydrogen desorption rate exceeds the silane adsorption rate, resulting in an emptying out of surface hydrogens. At lower temperatures, on the other hand, as the hydrogen desorption rate becomes comparable with the silane adsorption rate, part of the surface is covered with hydrogens. This indicates the possibility of the hydrogen desorption controlling the rate determining step at lower temperatures. Thus the suppressing effect that the presence of hydrogen in the gas phase has on the silicon growth rate can be explained by means of a competing and dissociative adsorption of hydrogen on the surface of the growing silicon layer.

Johnson et. al. [28] found that the (CH_3SiH_3, $(C_2H_5)_2SiH_2$, DTBS) molecules are first trapped in a precursor state, such as being physisorbed over H covered sites. From this precursor state, organosilane can diffuse across the surface until it either encounters a vacant Si or C site and dissociatively chemisorbs or, alternatively, desorbs from the surface. While accommodated at the surface, energy exchange between the organosilane and the surface phonons of the vibrationally excited chemisorbed layer can lead to bond cleavage or rearrangement reactions, with the resulting radical subsequently

being inserted into the surface Si-H or C-H bonds [28]. A higher fraction of hydrogen in the a-SiC:H films was found to be bonded to C. This may occur due to the increased carbon content as a result of the decomposition of the precursor into a greater number of carbon containing fragments at higher temperatures. The influence of hydrogen is such that it tends to form bonds with carbon thereby forming hydrocarbon molecules. The effect of hydrogen content is to decrease the relative amount of carbon in the condensed phase. This implies that carbon in the gas phase tends to bond preferentially to hydrogen when it is in sufficient quantities.

The density of the unoccupied bonds depends on the amount of hydrogen and therefore, at low temperatures, a lower density of states results from the higher degree of hydrogenation. As hydrogen desorbs from the film with the annealing process creating more unoccupied bonds, there is a trade-off between Si-C bond strengthening and hydrogenation. The hydrogen atoms bonding to carbon atoms cannot be removed as H_2 molecules as easily as can those bonding to silicon atoms. This is because the difference between H-H (435.9 kJ/mol) and C-H (413.3 kJ/mol) bond energies is less than that between the H-H (435.9 kJ/mol) and Si-H (294.5 kJ/mol) bond energies [36]. From the standpoint of carbon, the C-H bond is far stronger (413.3 kJ/mol) than any other combination with the exception of C=C bond (607.6 kJ/mol) which would be more important for situations low in hydrogen content [acetylene (C_2H_2)]. As a result many hydrogen atoms can be embedded into the amorphous structure at lower temperatures. At high temperatures some of the hydrocarbon species are not

incorporated into the amorphous network, but form stable hydrogen molecules on and/or near the substrate surface and desorb from the surface. Such a process may cause the reduction in the deposition rate of carbon atoms observed at high substrate temperatures. Within this framework, the rate-limiting step is dissociation of the precursor molecule, and hence the activation energy depends on the molecular structure and the nature of the radical fragments, in agreement with the experimental observations.

The hydrogen contained in the a-Si:H and in the a-C:H films is primarily bonded to tetrahedral (sp^3) Si and C atoms; however, depending on the deposition conditions, some of the hydrogen may be bonded to sp^2- and sp^1-coordinated atoms [37,38]. Nadler et. al. observed that after annealing, Si loses hydrogen and possibly forms sp^2 or sp^1 bonds. This does not cause a reduction of density of the film but an improvement of the Si-C lattice structure due to the replacement of weaker sp^3 bonds by stronger sp^2 or sp^1 bonds [39].

Stein and Habraken [40,41] observed that hydrogen is present in Si-H and N-H bonding configurations, of which the Si-H bond strength is the smallest. It is assumed that as the temperature increases the bonding between the Si-H weakens. Si bonds are created by burying incompletely bonded silicon atoms during growth, or by breaking buried Si-H bonds, either during deposition or in post deposition anneal. They observed that hydrogen also plays a very important role in the deposition of Si_3N_4 films, whether they are deposited at atmospheric pressure or low pressure. These bonds would give rise to increase in the charge transport thus resulting in increasing the deposition of silicon nitride films.

4.3 Deposition of Carbon and Silicon Species

Yoshimoto et. al. [36] observed that one of the weakest bonds is that of carbon and silicon because the bond strength of Si-C is 290 kJ/mol. Hydrogen atoms reaching the growing surface may etch out weakly bonded radicals such as C_2H_4, CH_3, and CH_2 resulting in a dense random network. There are no significant amounts of any gas species which carry both carbon and silicon. This suggests that each; C and Si, is deposited during separate reaction events. Thus it is not surprising that the predominant molecules bear either carbon or silicon in the gas phase but do not carry both. This also explains why reactants such as diethylsilane, ditertiarybutylsilane, and methylsilane breakdown at higher temperatures in forming simpler molecules.

Fischman et. al. [42] observed that silicon bearing species are geometrically asymmetric and therefore polar, whereas, carbon bearing species such as methane and acetylene are totally symmetric and, therefore nonpolar. This distinction is important when considering how the individual molecules interact with the deposition surface on impingement. Impinging polar molecules are likely to have greater "sticking" tendencies than nonpolar species when alignment and collision are favorable. This would be particularly true for molecules which consists of only partially satisfied configurations.

The amount of SiC deposited on the silicon wafer depends on C/Si ratio in the gas phase. As the ratio increases, increasing amounts of SiC codeposit with silicon. At ratios of ≈ 1, the system contains insufficient silicon and at this point

the maximum amount of silicon carbide is expected in the theoretically most stable situation [42].

4.4 Review of Deposition from Silanes

Current CVD processes used in the synthesis of reduced temperature deposits have traditionally relied on the use of silane (SiH_4) as a precursor for silicon bearing compounds. The deposition mechanism of silicon should have some similarities independent of the type of precursor used. A process can sometimes be better understood by extracting the common elements from many similar processes.

Eversteyn reported that the activation energy for the synthesis of silicon was found to be independent of the cholorosilane precursor used [29]. This observation could be explained if each precursor decomposed into the same species before or after surface incorporation or the reaction may be controlled by the desorption of some species. Silane pyrolytically decomposed into silicon and hydrogen. However the mechanism is very complex and many processing steps have to be considered [43]. The transport of the source gas to the wafer, adsorption or desorption of gas phase species on the wafer surface, or the transport of by-products away from the wafer can control the gas phase composition near the surface. There is also a possibility of the gas phase side reactions and deposition on the reactor walls in the region before the wafers; as heat is transferred to the input gases to raise their temperature to that of the furnace. Also as the gas flows without impedance through the annular region,

which lies between the wafer's edge and the reactor walls, there may be an exchange of gases between that region and the interwafer region through diffusion. The gases in the interwafer region are then adsorbed on the surface, a surface reaction occurs and the desorption of by-products such as hydrogen takes place. Finally, the by-product gases must diffuse to the annular region and be transported away. Thus, great care must be taken in any LPCVD study by taking into consideration the complex analysis and to ensure that the rate determining step is correctly identified.

Although it has been possible to deposit silicon films at low temperatures using silane as a precursor, it has its own limitations. Silane is pyrophoric (i.e. reacts when exposed to air) and highly reactive. When the silane concentration in the reactor is increased, homogeneous gas-phase decomposition takes place. Due to homogeneous gas-phase decomposition of silane, silicon particles are formed in the gas phase which can reach the growing silicon surface and in this way introduce crystalline imperfections.

The work of Lee and Kim [44] indicated that the growth rate of silicon from disilane is much faster than that of silane at the same temperature. It has been observed that disilane offers accelerated growth rates as compared to silane and improved wafer uniformity for low pressures in situ doping of p-type Si film grown with phosphine (PH_3) .

Johannes et. al. [45] observed that the growth rate of silicon containing species was dependent on the disilane partial pressure and temperature. One of the predominant dissociation channels for disilane pyrolysis is Si-Si bond

scission leading to SiH_2 and SiH_4. Disilane decomposition creates the SiH_2 and H_3SiSiH intermediates, and disilane reacts with these intermediates via the insertion reactions that generates the higher molecular weight silicon species. Also the formation of higher silanes, silenes and silylenes during disilane decomposition has been predicted. As the temperature increased above 640 K disilane decomposition increased, which led to increased formation of Si and higher molecular weight silicon containing species with the desorption of hydrogen [45]. Silicon from the molecular species that sticks on the surface may be incorporated into the silicon bulk, while the H_2 is evolved from the surface. To improve upon the disilane gas-phase mechanism, fundamental studies of rate constants and sticking coefficients are needed for the higher silanes, silenes, and silylenes. Also, when there is disilane depletion, less silane was available to intermediates and undergo insertion, resulting in the decrease in the growth rate of silicon.

4.5 Silicon Carbide Synthesis from Organosilanes

Investigations have been carried out for the incorporation of silicon into SiC, Si_3N_4 and Si-C-N films from various organosilane sources. It has been observed that the Arrhenius activation energy for the synthesis of silicon carbide and silicon nitride films have an activation energy (165-210 kJ/mol) very close to the energy required to remove hydrogen from a hydrogenated silicon surface [26,27,28,39].

Diethylsilane (DES) with a chemical formula of $(C_2H_5)_2SiH_2$ is a safer alternate precursor with a flash point of -20°C and an autoignition temperature of 218°C. It is a colorless liquid with a vapor pressure of 207 torr at 20°C and is commercially available at 99% chemical purity. Grow et. al. [26] studied the growth kinetics of the silicon carbide films as a function of the processing parameters over the deposition temperature range of 650-900°C, total pressure in the range of 0.1 to 0.5 torr and flow rates in the range of 10 to 50 sccm using diethylsilane (DES) as a precursor. In the 600 to 700°C range, the growth rate was observed to follow an Arrhenius behavior with an activation energy of 171 kJ/mol [26]. A plot of log (growth) rate v/s. the inverse temperature resulted in a linear graph upto 700°C followed by a region of much reduced growth rate. In the lower temperature region, the growth rate increased linearly with the temperature, but there is decrease in the growth rate at higher temperatures. The observed value of the activation energy is identical to values reported in the synthesis of silicon films from SiH_4 [46]. This indicates that there may be some similarity in the deposition of the silicon species. There is a change in the reaction mechanism for the rate determining step as the temperature is increased. This change could be due to the onset of crystallinity or the presence of increased side reactions at higher temperatures leaving less DES deposition. Above 700°C, the change in the slope of the deposition rate may also reflect a combination of factors including the transition into the mass-transfer limited regime in the interwafer region and the adsorption of decomposition products which retards the deposition process [47]. The observed monotonic increase in

the carbon content reflects the increase in the breakup of the Si-C bond at higher temperatures. The homolytic cleavage of Si-C was noted to be negligible below 725°C but to be important at higher temperatures. The availability of this additional source of carbon enhances the adsorption on the surface, thus causing the observed increase in the carbon content. Thus, it has been observed that the composition of the deposit shows a significant temperature dependence.

Grow et al. [26] have also studied the growth rate of silicon carbide as a function of total chamber pressure. At low pressures, as the chamber pressure increased, the growth increased in a linear manner typical of a first order mechanism. At higher pressures (above 0.2 torr) and a deposition temperature of 700°C, a saturation in the growth rate occurred indicative of the zero order process. Such a behavior is similar to that reported for the silicon synthesis from silane and may be considered to be consistent with a Langmuir-Hinshelwood mechanism where the growth rate for low pressure deposition is given by [48]:

$$\text{Rate} = kKp_{DES} / (1 + Kp_{DES}) \qquad (5.1)$$

where k is the reaction rate constant and K is the adsorption equilibrium constant

Although good quality amorphous films have been produced from diethylsilane with a wide range of stoichiometries, the resulting films were highly tensile and exhibited undesirable cracking. Ditertiarybutylsilane (DTBS) is also a safe alternate precursor to SiH_4 with a flash point of 15°C. It is a colorless liquid with a boiling point of 128°C, vapor pressure of 20.5 torr at 20°C, and is

commercially available with a 99% + chemical purity . Grow et. al. [27] proposed that there is a linear variation in the deposition rate as a function of square root of DTBS flow rate at constant conditions of temperature (650°C) and pressure (0.2 torr). This change can be explained if the bulky t-butyl groups require two sites, the necessity of gas phase reaction, or even in terms of transport phenomena. A Langmuir-Hinshelwood mechanism was observed. The deposition rate is seen to follow an Arrhenius behavior in the range of 600-675°C with an activation energy of 100 kJ/mol. The observed linear dependence can be explained by recognizing that the rate of laminar flow in the annular region can influence the partial pressure of DTBS in the interwafer region. As the DTBS flow rate in the annular region increases, the pumping rate in this region will increase accordingly to maintain the desired constant pressure. This will result in the removal of the by-products and will result in an increasing partial pressure of DTBS in the interwafer region until it reaches a maximum concentration. The composition of the deposits was observed to change from silicon rich to carbon rich between 650 to 800°C. As the temperature increases, the bonding of the molecule weakens and breaks down to silicon and carbon containing species. The quantity of the carbon containing species will be higher because of the presence of the ditertiarybutyl group, which undergoes decomposition at higher temperatures. With the use of DTBS the composition of the deposit is near stoichiometry at 750°C, while at higher temperatures, the films become progressively carbon rich while still remaining amorphous. It is, thus, apparent that the excess carbon present in the case of DTBS has the effect of quenching

the onset of crystallization and causing a reduction in the strength of the material [49].

Other studies on the deposition of silicon carbide from organosilanes have appeared in the literature. Several authors have studied the synthesis of silicon carbide from methylsilane [30,50]. The work of Johnson et. al. [28] indicated silicon carbide thin films have been deposited on silicon substrates from a single source reagent methylsilane (CH_3SiH_3). The source contains the constituent atoms Si and C; hence the SiC composition will to a large extent be controlled by their deposition chemistry along with process variables such as temperature, flow rate and pressure. Thermal decomposition kinetics have been studied in a low pressure (50 mTorr), cold wall CVD reactor over the temperature range 600-1150°C. It has been observed from the X-ray diffraction data that the film deposited from CH_3SiH_3 is crystalline above 750°C. The SiC film deposited from CH_3SiH_3 is Si-rich (C/Si = 0.8) at all temperatures and the activation energy is found to be 222 kJ/mole [28].

For homogeneous decomposition, the gas temperature near the substrate will determine the deposition which is dependent on both the substrate temperature and the gas-phase temperature gradient. It has been observed that the defect concentration is highest at the film/substrate interface and decreases with distance away from the interface. Although no surface carbonization step and no halogenated compounds were used, the deposition rates of the SiC films are in the range 0.1-1 μm/h and they were found to increase with increasing temperature.

The residence time of CH_3SiH_3 and H_2 affects the deposition rate. The residence time of CH_3SiH_3 and H_2 can be measured by monitoring the decay of their partial pressures after interrupting the gas flow. It was observed that the residence time of pure CH_3SiH_3 (50 mTorr, 5sccm) was 4s, while that for pure H_2, with the same exhaust valve position, was only 1.7s [28]. Identical values of the residence time of the components indicated the experimental conditions were found to be in the viscous flow regime.

As discussed earlier, in the low temperature regime (600 - 700 °C) of a low-pressure CVD reactor, deposition results primarily from surface reactions. The surface reaction probability β is defined as the fraction of the organosilane molecules that decompose and leave a bound Si atom at the substrate. Measurements of the surface reaction probability of SiH_4 have resulted in a better understanding of polycrystalline silicon LPCVD [51-53]. For SiH_4 decomposition, it has been established that the rate determining step of the mechanism is creation of surface H_2. This behavior is consistent with the mechanism where CH_3SiH_3 decomposition is controlled by the surface H coverage. The hydrogen content has been observed to decrease from 60% to 20% over the temperature range 600-1150°C. When the gas-phase decomposition of CH_3SiH_3 occurs, the adsorbed radicals $HSiCH_3$ and $H_2C = SiH_2$ can build the SiC network by inserting into the Si-H or C-H surface bond with subsequent H_2 elimination. The detection of CH_4 and SiH_4 as gaseous products of CH_3SiH_3 decomposition indicates that there is also some degree of Si-C bond breaking in the adsorbed state. Recent studies [54,55,] have shown that silylene

formation amounts to 10-15% of the total primary dissociation products over this temperature range. This can account for the silicon-rich films observed using CH_3SiH_3. The deposition rate of CH_3SiH_3 has been observed to follow Arrhenius behavior upto 1060K [50]. As the temperature increases, the growth rate increases linearly and the dependence of the growth rate on the growth temperature is expressed well by the Arrhenius equation. This means that the chemical reaction is the rate limiting-step for the crystal growth at lower temperatures. The value of the activation energy is observed to be 222 kJ/mole [28]. At high temperatures, the growth rate is almost independent of the growth temperature. This relation indicates that the growth rate is limited by the transportation of a reactant in the gas phase under the growth condition.

Grow et. al. [39] have also determined the growth kinetics of silicon nitride (Si_3N_4) films as a function of the processing parameters using TDMAS and NH_3 as precursors over the deposition temperature range of 650 to 900°C and total pressure in the range of 0.15 to 0.60 torr. They observed that the growth rate is seen to follow an Arrhenius behavior that yields an apparent activation energy of 171-184 kJ/mol in the range of 650 to 800°C. It was also observed that above 800°C, a combination of factors including enhanced homogeneous reactions and depletion effects resulted in lower growth rates. They found that the growth rate varied linearly with the total pressure and was in agreement with the Langmuir-Hinshelwood mechanism. The FTIR spectrum revealed the presence of hydrogen at lower temperatures where Si-H and N-H bonds were detected.

Bean et. al. [56] reported that the growth rate for the SiH_4-NH_3-H_2 is seen to follow an Arrhenius behavior that yields an apparent activation energy of 217 kJ/mol. The film thickness uniformity across the reaction chamber was excellent reflecting the lack of depletion effects in the range of 650 to 750°C. It was observed that at higher temperatures the growth decreased due to a combination of factors including enhanced gas phase nucleation and depletion effects as observed during the deposition of silicon. Bean et. al. determined the effect of temperature on deposition rate for different silane concentrations. A change in the deposition mechanism is observed around 900°C and the apparent activation energy drops to around 104 kJ/mol. There is a possibility that the change in the activation energy may occur due to the decomposition of silane before it reaches the substrate or the decrease in the activation energy may mark the entrance in diffusion controlled reaction which would be expected to be nearly temperature insensitive. Similar behavior has been observed in the deposition of silicon films from silanes. This indicates that there is a possibility that the hydrogen desorption may play an important role at lower temperatures in the mass transport regime and Si_3N_4 absorption may be significant at higher temperatures during the diffusion controlled regime. The transport of hydrogeneous species during thermal nitridation of silicon films is determined by means of isotopic tracing of hydrogen. It is well known that when hydrogen is not contained in the nitriding molecule, during thermal treatments of molecules, incorporation of nitrogen in the film does not occur [57]. However, it has been proposed that hydrogen is not only an element in the ammonia (NH_3) molecule, a molecule

which is thermally dissociated much more readily than the N_2 molecule, but is also a component of the nitrogen species adsorbed on the Si surface and participates in the transport of the nitriding species from the film surface towards the interface. The role of nitrogen uptake is driven by the diffusion and reaction of NH_2 in the film. NH_2 and NH radicals are also diffusing species that promote, at least partially, the nitridation of the silicon films. Recent in situ experiments demonstrated that amines are dissociatively adsorbed at the surface of Si(100), producing NH_2 and H, and that NH_2 molecules are further dissociated giving NH and H [58].

CHAPTER 5

RESULTS AND CONCLUSIONS

5.1 Deposition of Silicon Carbonitride Films

Silicon carbonitride films have been deposited by the use of an environmentally benign silicon precursor; tri(dimethylamino)silane (TDMAS), which has chemical formula $((CH_3)_2N)_3SiH$ and a molecular weight of 161 and specific gravity of 0.8. From an environmental standpoint, it is nonpyrophoric, nonexplosive, and a noncorrosive liquid with a boiling point of 145°C and a flash point of 25°C. It has a vapor pressure of 5 torr at 25°C and is commercially available with a 99% + chemical purity . Olin Chemicals provided us with this novel precursor . However, it was available in limited quantities because it is a unique material. Initially a study was made on the chemical vapor deposition of silicon nitride using TDMAS and NH_3 by Grow et al. [39]. This precursor is prepared only by Olin Chemicals and so we carried out the experimental runs at selected temperatures, pressures and flow rates because of its limited availability.

Using TDMAS as a precursor, the growth kinetics of the film were determined as a function of the processing parameters over the deposition temperature range of 650-850°C, total pressure varying from 0.2-0.5 torr and TDMAS flow rates at 10 and 20 sccm. Initially, the deposition was carried out at 650°C, with a pressure of 0.5 torr and a flow rate of 10sccm. The growth rate was found to be 22 Å/min. The deposition temperature was increased to 750°C, keeping the pressure and flow rate constant. As the temperature increased, the

decomposition of TDMAS increases which leads to a higher growth rate. The growth rate was found to vary between 140-150 Å/min. The silicon carbonitride film was then deposited at a temperature of 700°C, at a pressure of 0.5 torr and a flow rate of 20 sccm. The growth rate was found to be around 45-55 Å/min. However, the presence of homogeneous gas phase nucleation could be seen because the reaction was carried out at a higher pressure. At lower deposition pressures of 0.2 torr the silicon carbonitride film was found to be uniform with growth rates around 40 Å/min. Above 750°C, the growth rate was observed to decrease with increasing temperature, reflecting a combination of factors including enhanced gas phase nucleation and depletion effects. At 850°C, and a pressure of 0.5 torr and flow rate of 10 sccm, the growth rate was observed to decrease significantly to around 50 Å/min. This decrease in the deposition rate may also occur due to the difficulty of measuring film thickness by ellipsometry because of non-uniformity of the surface. The energy striking the surface is scattered, and only a portion is returned to the ellipsometer detector. The silicon carbonitride film was found to be uniform when the flow rate was decreased from 20 sccm to 10 sccm keeping pressure constant at 0.5 torr and temperature varying from 650-750°C. The growth rate varied between 30 -120 Å/min over this temperature range.

Figure 5.1 illustrates the variation in growth rate as a function of temperature at a constant total pressure of 0.5 torr and TDMAS flow rate of 10 sccm. In the range of 650 to 750 °C, the growth rate is consistent to follow an Arrhenius behavior that yields an apparent activation energy of 175 kJ/mole. This

value can be compared to the silicon carbonitride deposition from NH_3/TDMAS which was observed to follow an Arrhenius behavior in the temperature range of 650-800°C with an activation energy of 171-184 kJ/mol as reported by Grow et. al. [39]. Also the silicon carbide film deposited from diethylsilane was observed to follow an Arrhenius behavior in the range of 600-700°C with an activation energy of 171 kJ/mol as reported by Grow et. al [26]. This indicates that there is a possibility of some common mechanism controlling the deposition rate at low temperatures. One of the possibilities is that the silicon adsorption rate may be an important rate controlling parameter.

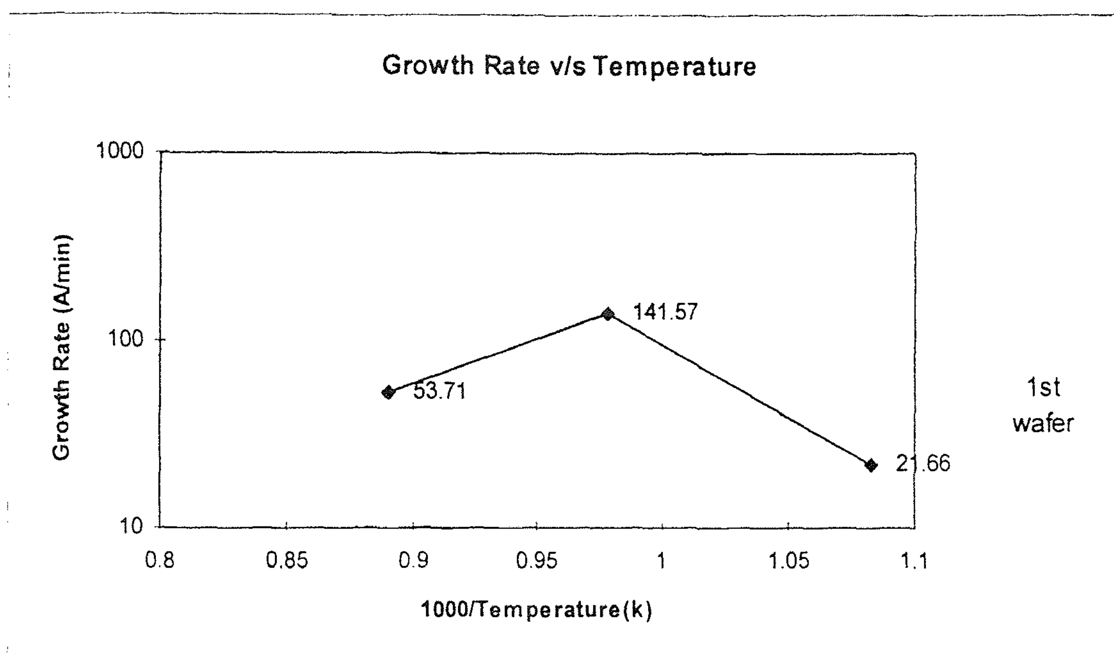

Figure 5.1 Dependence of growth rate on temperature

The decrease in the deposition rate may mark the entrance into a diffusion controlled reaction which would be expected to be temperature sensitive. Also as the temperature increases, TDMAS undergoes decomposition into species containing carbon, nitrogen and silicon. This will also result in the

decrease in the partial pressure of TDMAS being deposited. The rapid decrease in the growth rate with higher deposition temperatures is similar to that reported for the SiH_4-H_2-NH_3 system [56]. The growth rate for the SiH_4-H_2-NH_3 system was observed to follow an Arrhenius behavior with an activation energy of around 209 kJ/mol at lower temperatures and the activation energy was found to decrease to around 25 kJ/mol at higher temperatures. The presence of the amino group in TDMAS results in the deposition of a silicon nitride film. It has been observed that the films deposited with low amine concentration are found to be silicon rich. It is also interesting to note that the deposition rate at low amine concentration approaches the silicon deposition rate from pure silane in the reactor.

5.2 Characterization of Silicon Carbonitride Films

5.2.1 Film Compositon

The composition of the film was found to remain constant at temperatures of 700 and 750°C. Preliminary results have shown that TDMAS produces a silicon carbonitride film consisting of nearly equal amounts of silicon carbide and silicon nitride. The results of the XPS data for 0.5 torr pressure, 750°C and a flow rate of 10 sccm are shown in figure 5.2. The XPS data revealed the presence of oxygen at concentration levels near 3% in the form of impurities incorporated in the film. The carbon content in the silicon carbonitride film was found to be 25% and the the nitride composition was also found to be 25%. The silicon line in the XPS spectra is narrow and symmetric showing a composition of 47%.

Figure 5.2 ESCA profile of silicon carbonitride film at 750°C, pressure of 0.5 torr and flow rate of 10sccm.

The observed binding energy of silicon (101.6 eV), was higher than that of SiC (100.2 eV), and close to that of Si_3N_4 (101.8 eV). The observed binding energy of nitrogen (399 eV) was higher than that of Si_3N_4 (397.6 eV), reflecting the presence of carbon and oxygen species. The presence of carbon occurs due to the deposition of TDMAS on the siliocn wafer. The presence of oxygen occurs due to the residual gas present within the reactor. The observed binding energy of carbon (283.2 eV) indicates the presence of characteristic carbon in carbides [59,60]. No traces of hydrogen have been detected in the XPS spectra at this temperature. This indicates that hydrogen has been completely desorbed from the film. The XPS analysis for 0.2 torr pressure, 700°C and flow rate 20 sccm indicated the composition as shown in figure 5.3. Here the concentration of oxygen increases to about 9%. This is because of the presence of the oxygen in

the residual gases within the reactor which gets deposited on the film at high temperatures reacting with the silicon wafer. The carbon content in the silicon carbonitride film was found to be 23% and the nitride content was observed to be 24%. The silicon line in the XPS spectra shows a composition of 44%. The presence of the direct single Si-N bonds and lack of direct Si-C bonds in the structure of this molecule is expected to enhance the formation of stoichiometric Si_3N_4.

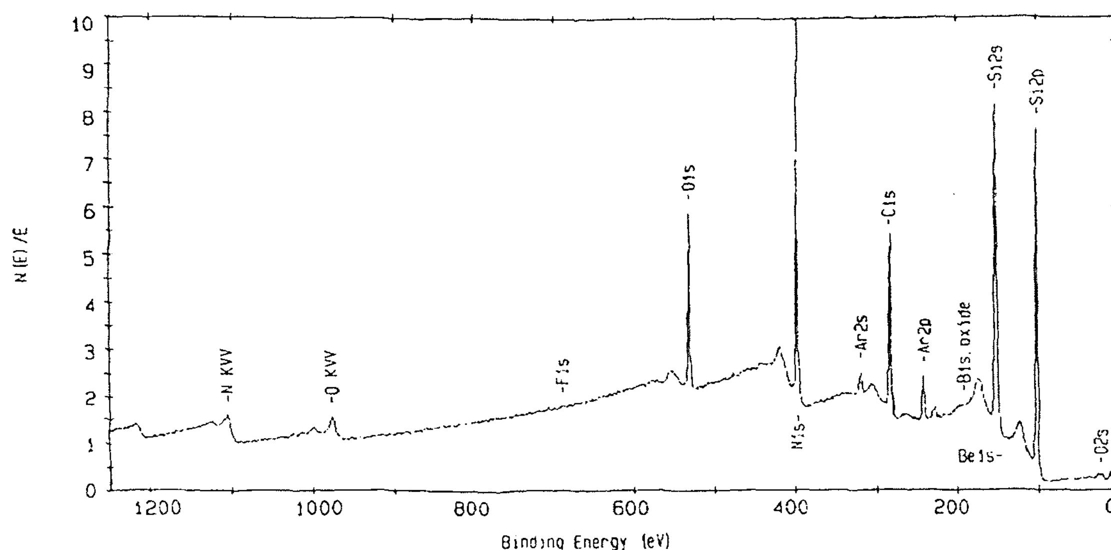

Figure 5.3 ESCA profile of silicon carbonitride film at 700°C, pressure of 0.2 torr and flow rate of 20sccm.

In synthesizing good quality Si-C-N films, heterogeneous reactions must occur. However, some portions of the overall reaction may occur in the gas phase. SiC and Si_3N_4 molecules adsorbed on the Si wafer surface diffuse randomly and have a greater opportunity to desorb because they are less firmly bound to the substrate. As the adsorbed molecules diffuse on the surface, they

encounter other diffusing molecules and form a pair. The molecule pair would be more stable than an isolated molecule and would less likely be desorbed. Because the probability of diffusing molecules encountering each other depended strongly on the number of the adsorbed molecules on the surface, it is a strong function of the arrival rate (pressure of the precursor) and the desorption rate (temperature of the substrate and the binding energy of the diffusing molecules).

5.2.2 Density

The density of the Si-C-N films was determined from the thickness (as measured on the polished side of the wafer) and the total mass of the deposit over these wafers. In cases where film deposition occurred on both sides of the wafer, the film thickness on the nonpolished side of the wafer was assumed to be the same as that on the polished side. This assumption is justified in view of the minimal depletion effects encountered in this process. Grow et. al. [26] observed the density of SiC films to be around 2.2 gm/cc when deposited from diethylsilane. The density of SiC using di(tertiary)butylsilane was found to be 2.0 gm/cc [27]. Grow et. al [39] reported the density of Si-C-N film as 2.3 gm/cc for carbon rich films and 2.56 gm/cc for films rich in nitride content using NH_3/TDMAS as the precursor.

As seen in figure 5.4, the film density is observed to remain constant at 2.3 gm/cc which is consistent to indicate the presence of silicon carbide and silicon nitride deposition. This value is lower than the value of 3.2 gm/cc reported

for bulk SiC and 3.44 gm/cc for the bulk Si_3N_4 with the difference being accounted by the amorphous nature of the film [56]. This value is close to the densities of SiC and Si_3N_4 observed from recent studies.

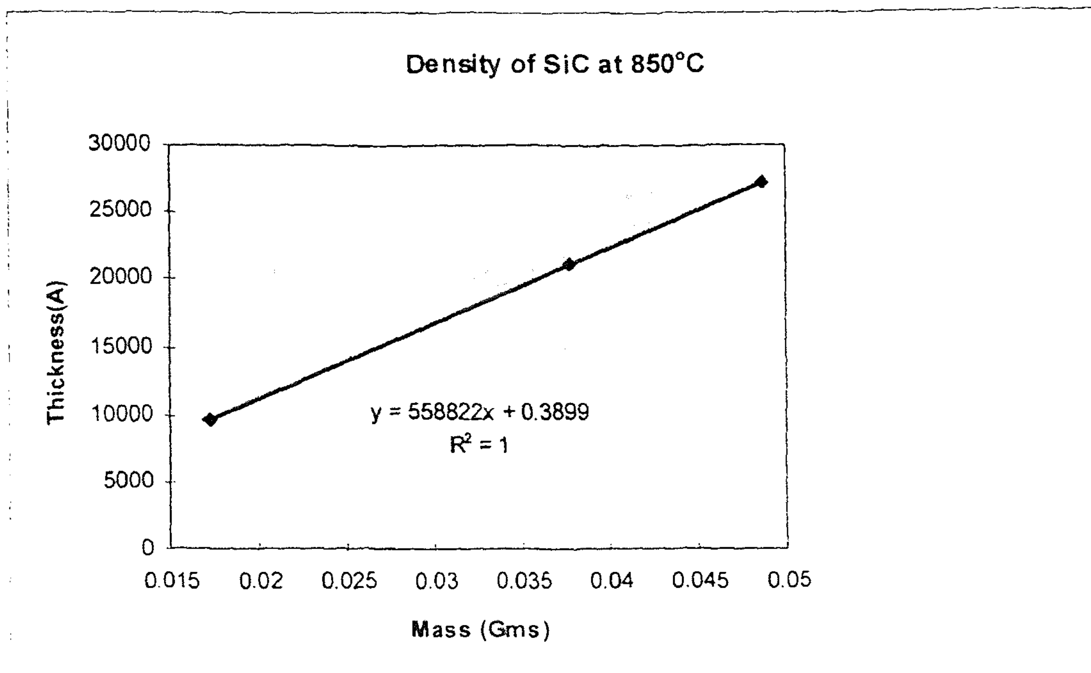

Figure 5.4 Density of silicon carbide at 850°C

The X-ray diffraction pattern of the Si-C-N films deposited indicated that the films are amorphous at the temperatures studied. The film stress was determined with a home built system that measured changes in the radius of curvature of the wafer resulting from deposition on a single side. The stresses were measured for films at different conditions of pressure and flow rate. The film stress was observed to have a value of 2.2 MPa at a temperature 700°C, a pressure of 0.5 torr and a flow rate of 20 sccm. The stress was found to be 4.51

MPa at a temperature of 700°C, a pressure of 0.2 torr and a flow rate of 20sccm. The films were found to be tensile in both cases.

5.2.3 Refractive Index

The refractive index was measured with a Rudolph Research Auto EL ellipsometer. It was measured over five different points on the surface of the wafer to ensure uniformity. The refractive index measurements were performed for four experimental runs. The deposition was carried out on four wafers for each run. At a temperature of 650°C, a pressure of 0.5 torr, and a flow rate of 10 sccm the refractive index was determined for two wafers. The other two wafers were broken while removing them from the reactor. The first wafer had a refractive index of 2.10 and the second wafer had a refractive index of 2.17. As the temperature increased to 750°C, keeping the pressure constant; the refractive index was determined for four wafers. The first two wafers had a refractive index of around 2.23.The last two wafers had a refractive index between 2.4-2.45. This indicates that the refractive index may increase with increasing temperature. The refractive index was also found to vary along the sides of the wafer. This may be possibly due to deposition of nitride on one side and that of carbides on the other.

At a temperature of 700°C, a pressure of 0.5 torr and a flow rate of 20 sccm, the refractive index was found to vary substantially. The first wafer had a refractive index of 2.15. The second wafer had a refractive index of 2.84. The third wafer was found to have a refractive index of 3.04. The fourth wafer had a

refractive index of 2.74 indicating the presence of SiC rich films. As the deposition pressure was reduced to 0.2 torr at constant temperature and flow rate, the refractive index for the first wafer was 2.03. The refractive index for the second and third wafer was around 2.14. The refractive index of the fourth wafer was 2.21. This indicates that there is a possibility that the refractive index may decrease with the increase in pressure. Grow et. al. [27] reported the refractive index for the silicon carbide film deposited from DTBS as 2.7. Grow et. al. [39] reported a value of 2.37 for carbon rich films and a value of 2.00 for nitride rich films.

5.2.4 Fourier Transform Infra Red Spectroscopy (FTIR)

The FTIR spectra were taken using a Perkin-Elmer 1600 series spectrophotometer. The 820 cm^{-1} band indicates the presence of the Si-C-N film. The presence of this broad centered peak lies between 780 cm^{-1} (wavenumber for the Si-C vibrational mode) and 830 cm^{-1} (wavenumber for the Si-N vibrational mode).The 475 cm^{-1} band is associated with bond vibrations of nitrogen perpendicular to the Si-C-N planes but these modes extended spatially throughout the whole network.

The vibrations are characterized by much lower frequencies than the stretching modes which involve large force constants [61]. The presence of N-H bonding (about 1475 cm^{-1}) and N-H (3345 cm^{-1}) indicates a number of hydrogen atoms bond to nitrogen in the film at 700°C. The adsorption band at 2160 cm^{-1} is assigned to the stretching mode of Si-H bonding.

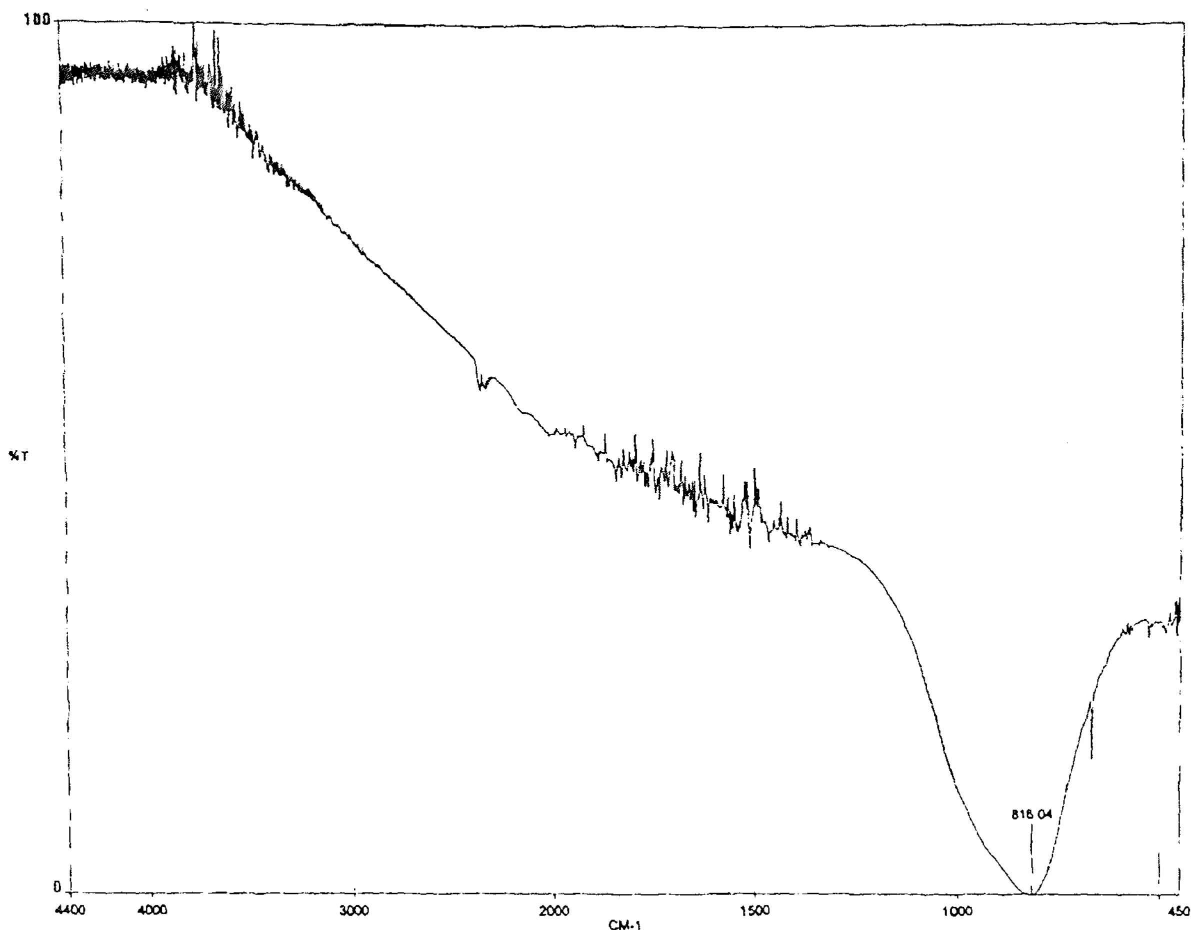

Figure 5.5 FTIR spectrum for silicon carbonitride film at a temperature of 700°C, pressure 0.2 torr and flow rate 10sccm.

It seems that the Si-H bond has been broken at this temperature due to the weak Si-H bonding.

It seems from figure 5.6 that the Si-C-N film has been oxidized and the film appears to be thicker than the one deposited at 0.2 torr. Hydrogen plays an important role in the electrical performance of Si_3N_4 films. The integrated absorption of the N-H and Si-H bands are correlated with the atomic concentration of hydrogen. The position of the Si-N stretching and breathing modes are sensitive to Si-H content; their absorption peaks being shifted to

relatively higher wave numbers indicates an increasing number of hydrogen atoms bonded to a specific Si atom, especially when the Si atoms are incorporated with the N atoms, whose electronegativity is greater than that of Si atoms [62]. Recent studies [26,27,39] also reported the presence of Si-H bonds which indicates that hydrogen desorption may be the rate controlling step. The presence of carbon dioxide in the films is indicated by the peak appearing at 2340 cm^{-1}.

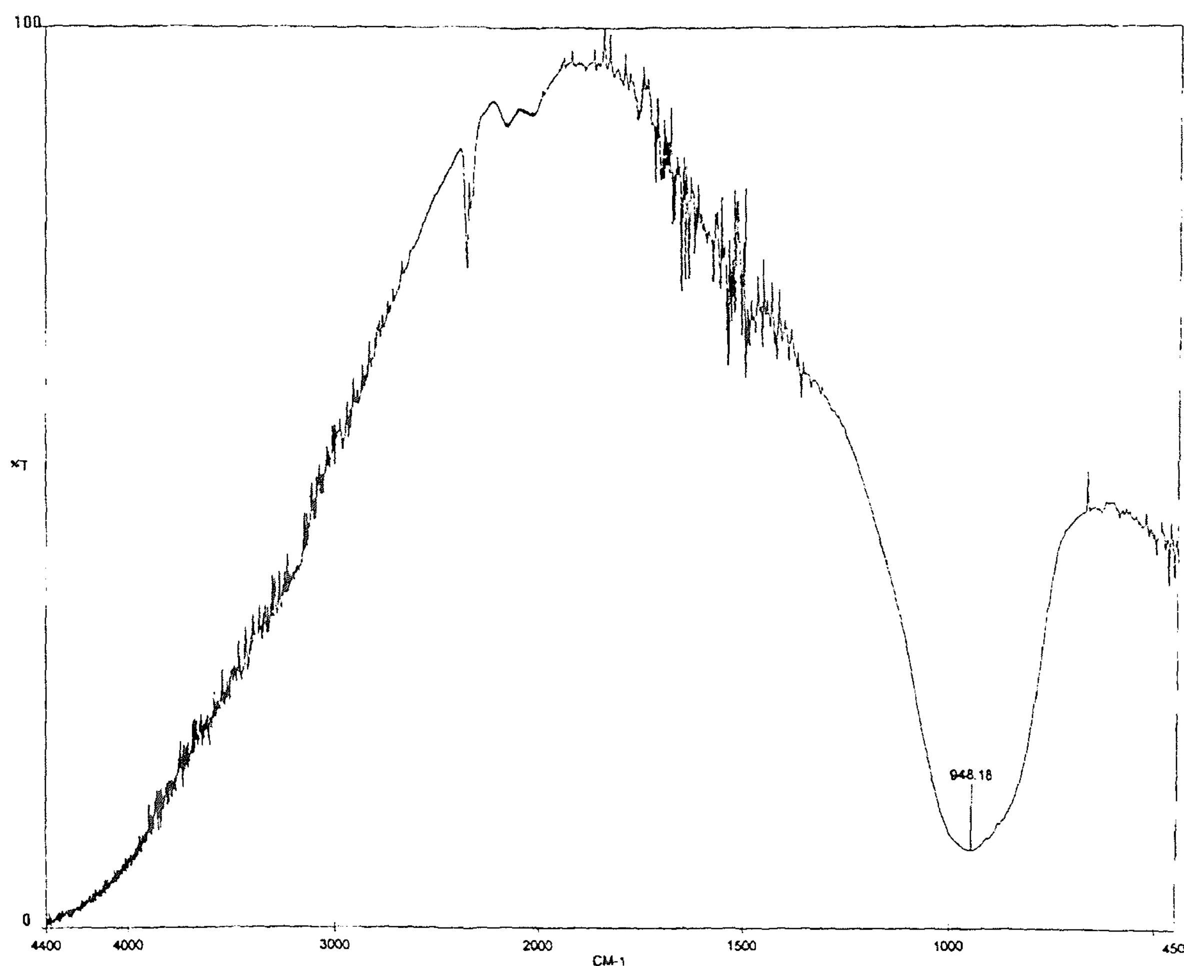

Figure 5.6 FTIR spectrum for silicon carbonitride film at a temperature of 700°C, pressure 0.5 torr and flow rate 20sccm.

5.2.5 Young's Modulus of Silicon Carbonitride Film

The hardness of the Si-C-N film was determined using a Nanoindenter.

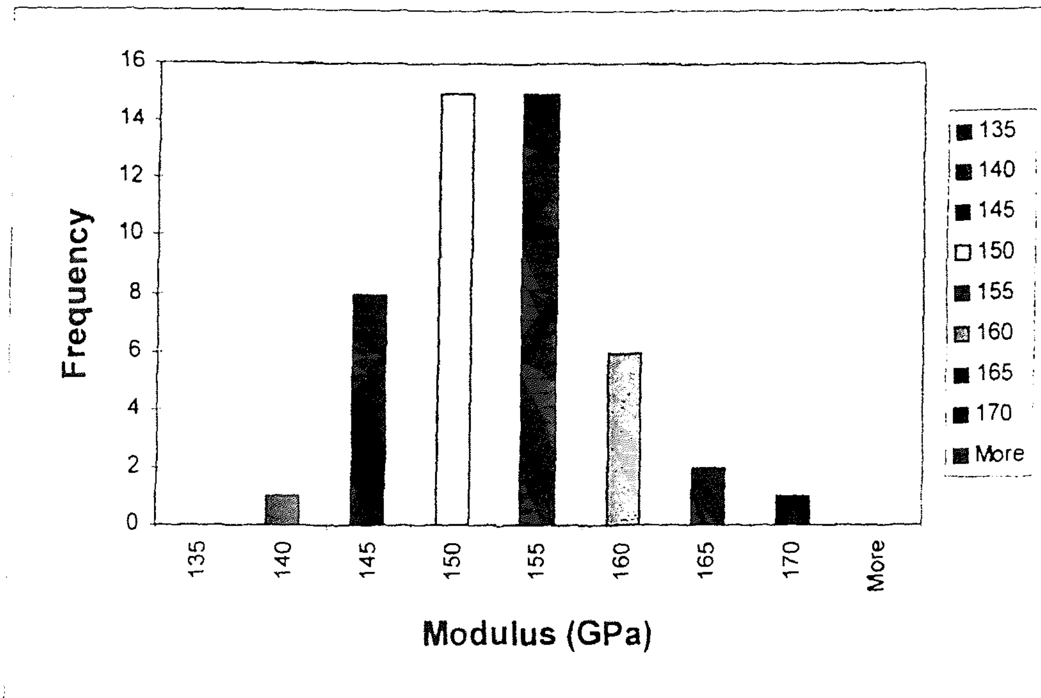

Figure 5.7 Young's Modulus of silicon carbonitride films at 700°C.

The figures 5.7, 5.8 and 5.9 represent the plots of Young's modulus as a function of deposition temperature. It is observed that in figures 5.7 and 5.8 there appears to be an increase in these values as the deposition temperature is raised upto 750°C. This increase may be due to the increase in the carbonitride content until the stoichiometric value for the composition is reached. At 700°C the value of Young's modulus was found to be around 150 Gpa from figure 5.7. At 750°C, the value for Young's modulus was close to 185 Gpa as can be seen from figure 5.8.

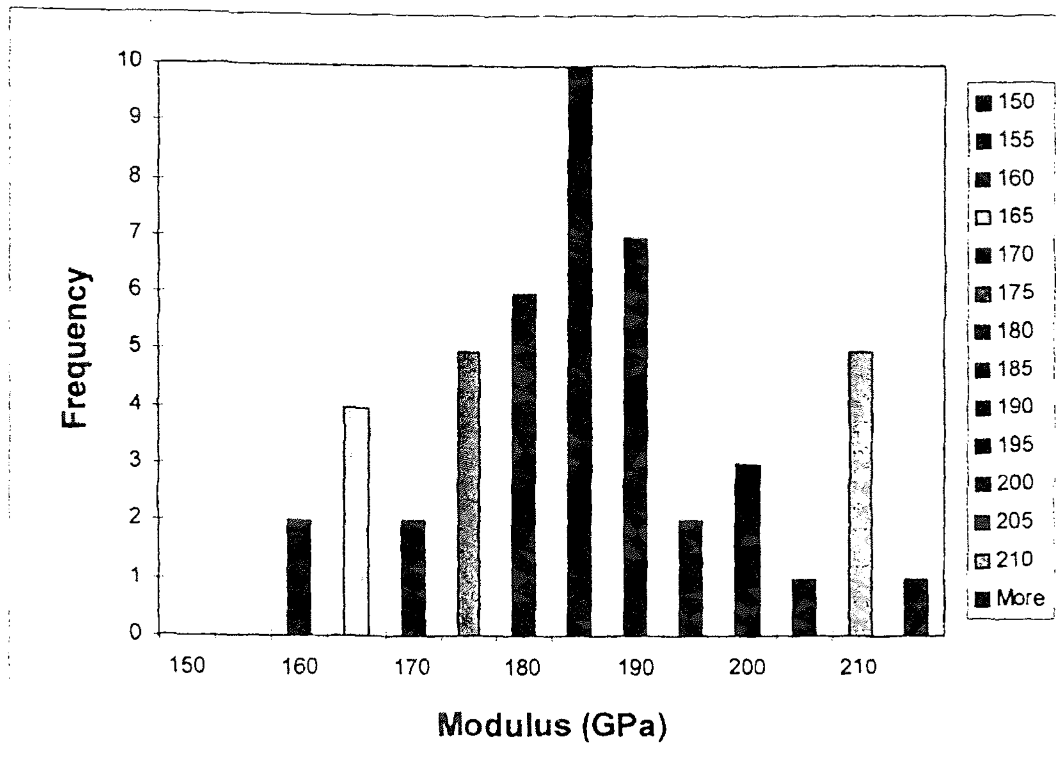

Figure 5.8 Young's Modulus of silicon carbonitride films at 750°C.

The Young's modulus of these films produced at deposition temperatures above 800°C do not increase in value with deposition temperatures and multiple measurements of films produced at this higher temperature do not follow a normal distribution as observed by the films produced at lower temperatures as shown in figure 5.9. This decrease in the value for the Young's modulus may reflect the deviation from stoichiometry and increased presence of carbonitride in the neutral state. It may also indicate the presence of non-homogeneous materials at high deposition temperatures.

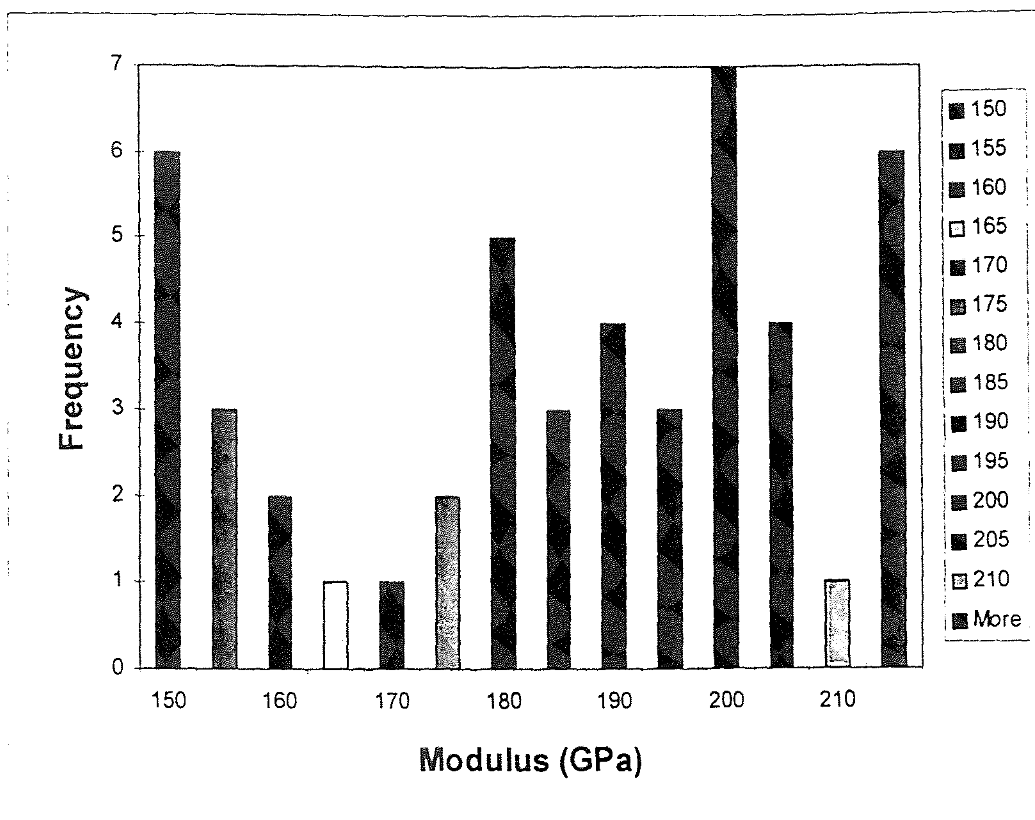

Figure 5.9 Young's Modulus of silicon carbonitride films at 850°C.

5.3 Conclusions

Amorphous high quality stoichiometric Si-C-N films were synthesized on silicon wafers by low pressure chemical vapor deposition from tri(dimethylaminosilane) TDMAS in the temperature range of 650 - 850°C. The temperature dependent behavior of deposition rate is consistent with Arrhenius behavior in the low temperature range (650-750°C) with an activation energy of around 175 kJ/mol. This indicates that there is a possibility that there may be some common mechanism influencing the deposition of organosilanes such as diethylsilane, ditertiarybutylsilane, methylsilane and TDMAS. The activation energy of the carbides and nitrides from silanes and organosilane has been observed to lie in

the range of 165-210 kJ/mol. This value corresponds to that of silicon deposition with the loss of hydrogen taking place. One of the possibilities is that the desorption of hydrogen may be the rate controlling step at lower temperatures.

For precursor mediated decomposition, the vacant sites occupied by hydrogen influences the surface reaction probability by controlling the rate of direct absorption of chemical species at a vacant site and the diffusion length of the precursor. At high temperatures, therefore, when the sites occupied by hydrogen are low, there is expected to be a decrease in the apparent activation energy for the organosilane decomposition. It has also been observed that the rate of silicon deposited increases as the temperature increases and maybe an important rate controlling factor in the deposition of carbides and nitrides. Thus it is possible that the silicon deposition rate and the rate at which hydrogen desorbs maybe the rate controlling factor in the deposition of SiC and Si-C-N species.

The X-ray diffraction patterns indicate the amorphous nature of as-deposited silicon carbonitride films. The bulk density was found to be 2.3 gm/cc which takes into account the amorphous nature of the film. The ESCA analysis determined the composition of the individual species in the silicon carbonitride film. The carbide and the nitride content was found to be remain constant independent of the deposition temperature. However, the optimum film synthesis was found to be at 750°C, at a pressure of 0.5 torr and flow rate of 10sccm.

REFERENCES

1. Wolf, S. and Tauber, R. N., *Silicon Processing for the VLSI Era, Volume1: Process Technology*, Lattice Press, Sunset Beach, California (1991)

2. Nolang, B., "Equilibrium Computations and Their Application to CVD Systems," *Proceedings of 5th European Conf. on CVD*, 107-115, University of Uppsala, Sweden (1985).

3. Erikson, G., *Acta Chem. Scandia*, 25, 2651-2658 (1971).

4. Besmann, T. M., SOLGASMIX-PV, "A Computer Program to Calculate Equilibrium Relationship in Complex Systems," ORNL/TM-5775, *Oak Ridge National Laboratory*, Oak Ridge, TN (1977).

5. Spear, K. E., "Thermochemical Modeling of Steady-State CVD Process," *Proc. 9th. Int. Conf. on CVD*, Electrochem. Soc., 81-97, Pennington, NJ 08534 (1984).

6. Pierson, H. O., *Handbook of Chemical Vapor Deposition*, Noyes Publications, Park Ridge, New Jersey (1992).

7. Nakajima, N., Jimbo, H., and Watanabe, A., *Proceedings of 9th European Conf. on CVD*, Electrochemical Society, Pennington, NJ, 257 (1989).

8. Deschamps, A., Walther, C., Beragez, P., and Charpin, J., *Proceedings of 9th European Conf. on CVD*, Electrochemical Society, Pennington, NJ, 237 (1989).

9. Ohring, M., *The Materials Science of Thin Films*, Academic Press, San Diego, California (1992).

10. Galasso, F. S., *Chemical Vapor Deposited Materials*, CRC Press, Boca Raton, Florida (1991).

11. Yoder, M. N., "Wide Bandgap Semiconductor Materials and Devices," IEEE Transactions on Electron Devices, Vol. 43, 1633-1636 (October 1996).

12. Harris, G. L., and Yang, C.W., "Amorphous and Crystalline Silicon Carbide," Springer Proceedings in Physics, Vol.34, Springer-Verlag, New York (1989).

13. Harris, G. L., Yang, C.W., and Rahman, M. M., "Amorphous and Crystalline Silicon Carbide," Springer Proceedings in Physics, Vol.43, Springer-Verlag, New York (1989).

14. Kern, W., and Ban, S. V., *Thin Film Processes*, Academic Press, New York (1978).

15. Blocher, M. J. Jr., *Deposition Technologies for Films and Coatings: Developments and Applications*, Noyes, New Jersey (1982).

16. Ojha, S. M., *Physics of Thin Film*, Vol.12, Academic Press, New York (1982).

17. Thornton, J. A., *Deposition Technologies for Films and Coatings: Developments and Applications*, Noyes, New Jersey (1982).

18. Bonifield, T. D., *Deposition Technologies for Films and Coatings: Developments and Applications*, Noyes, New Jersey (1982).

19. Catherine, Y., "Proceedings 5th Symp. on Plasma Processing", *Journal of Electrochemical Society*, Vol. 85-1, 317, (1985).

20. Sugano, T., *Applications of Plasma Processes to VLSI Technology*, Wiley & Sons, New York (1985).

21. Chen, J. Y., and Henderson, R., "Photo - CVD for VLSI," J. Electrochem. Soc., Vol. 131, 2147, (September 1984).

22. Solanki, R., Moore, C., and Collins, G., "Laser Induced CVD," *Solid State Technol.* Vol. 220, (June 1985).

23. Bhaskaran, M., "Synthesis and Characterization of LPCVD Silicon Carbide Thin Films for X-Ray Lithography," Thesis, Department of Electrical Engineering, NJIT, Newark, New Jersey, (1991).

24. Smith, D.K., Barrett, C. S., Leyden, D. E., and Predecki, P. K., *Advances in X-Ray Analysis*, Vol. 24, Plenum Press, New York, (1981).

25. Seah, M. P., and Dench, A. W., *Surface Interface Analysis*, Vol. 1, 2, California, (1979)

26. Grow, J. M., Levy, R. A., and Shi, Y.T., "Low Pressure Chemical Vapor Deposition of Silicon Carbide from Diethylsilane," *Journal of the Electrochemical Society*, Vol. 140, No. 3, 851-854 (March 1993).

27. Grow, J. M., Levy, R. A., and Bhaskaran, M., "Low Pressure Chemical Vapor Deposition of Silicon Carbide from Ditertiarybutylsilane," *Journal of the Electrochemical Society*, Vol. 140, 3001-3007, No. 10, (October 1993).

28. Johnson, A. D., Perrin, J., Mucha, J. A., and Ibbotson, D. E., "Kinetics of SiC CVD: Surface Decomposition of Silacyclobutane and Methylsilane," *J. Phys. Chem.* Vol. 97, 12937-12948, (1993).

29. Eversteyn, F. C., "Chemical Reaction Engineering in the Semiconductor Industry," *Philips Res. Rep.*, Vol. 29, 45-66, (1974).

30. Golecki, I., Reidniger, F., and Marti, J., "Single-Crystalline Epitaxial Cubic SiC Films Grown on (100) Si at 750 °C by Chemical Vapor Deposition," *Appl. Phys. Lett.,* Vol. 60, 6, (1992).

31. Hirth, J., and Pound, G., *Condensation and Evaporation*, Pergamon: Oxford, U.K., (1963).

32. Gates, S. M., Greenlief, C. M., Beach, D. B., and Holbert, P.A., "Decomposition of Silane on Si(111) and Si(100) Surfaces Below 500°C," *J. Chem. Phys.*, Vol. 92, 3144, (1990).

33. Gates, S. M., Greenlief, C. M., Kulkarni, S. K., and Sawin, H. H., "Surface Reactions in Si Chemical Vapor Deposition from Silane," *J. Vac. Sci. Technol.* Vol.8, 2965, (1990).

34. Hirose, F., Suemitsu, M., and Miyamoto, N., "Surface Hydrogen Desorption as a Rate-Limiting Process in Silane Gas-Source Molecular Beam Epitaxy," *J. J. Appl. Phy.*, Vol. 29, L1881, (1990).

35. Gates, S. M., and Kulkarni, S. K., "Kinetics of Surface Reaction in Very Low Pressure Chemical Deposition of Si and SiH_4," Appl. Phys. Lett., Vol. 58, 2963, (1991).

36. Fujii, Y., Yoshimoto, M., Yamazoe, K., and Matsunami, H., "Preparation of Hydrogenated Amorphous Si-C Alloy Films and Their Properties," *Thin Solid Films,* Vol. 117, 59-69, (1984).

37. Nadler, M. P., Donovan, T.M., and Green, A.K., *Thin Solid Films*, Vol.116, 241, (1984).

38. Pankove, J.I., *Semiconductors and Semimetals, Hydrogenated Amorphous Silicon*, Vol. 21, Part A, 41-54, Academic Press, New York, (1984).

39. Grow, J. M., Levy, R. A., and Lin, X., "Low Pressure Chemical Vapor Deposition of Silicon Nitride using the Environmentally Friendly Tris(dimethylamino)silane Precursor," *Journal of Materials Research*, Vol. 11, No. 6, (June 1986).

40. Stein, H. J., and Wegener, H. R., "Chemically Bound Hydrogen in CVD Si_3N_4: Dependence on NH_3/SiH_4 Ratio and on Annealing," *J. Electrochem. Soc.*, Vol. 124, No. 6, 908, (June 1997).

41. Habraken, F. M., Tijhaar, R. G., and Weg, W. F., "Hydrogen in Low-Pressure Chemical-Vapor-Deposited Silicon (Oxy)nitride films," *J. Appl. Phys.*, Vol. 59, No. 2, 447, (January 1986).

42. Fischman, G.S., and Petuskey, W. T., "Thermodynamic Analysis and Kinetic Implications of Chemical Vapor Deposition of SiC from Si-C-Cl-H gas systems," *J. Am. Ceram. Soc.*, Vol. 68, No. 4, 185, (1985).

43. Purnell, J.H., and Walsh, R., "The Pyrolysis of Monosilane," *Proc. Roy. Soc.,* Vol. 293, 543, (1966).

44. Lee, E. G., and Kim, J.J., "Investigation of Microstructure and Grain Growth of Polycrystalline Silicon Deposited Using Silane and Disilane," *Thin Solid Films*, Vol. 26, 123, (1993).

45. Johannes, J. E., and Ekerdt, J.G., "Gas-Phase Reaction Study of Disilane Pyrolysis: Applications to Low Pressure Chemical Vapor Deposition," *J. Electrochem. Soc.*, Vol. 141, No. 8, 2135, (1994).

46. Claassen, W. P., Bloem, J., Valenburg, W. J., and van den Brekel, C. J., *J. Crystal Growth*, Vol. 51, 267, (1982).

47. Kern, W., and Levy, R. A., *Microelectronic Materials and Processes*, 203, Kulwer Academic Publishers, Boston, MA (1989).

48. Laidler, K. J., *Chemical Kinetics*, 226, McGraw Hill, Inc., New York, (1965).

49. Grow, J. M., and Levy, R. A., "Micromechanical Characterization of Chemically Vapor Deposited Ceramic Films," *Journal of Materials Research*, Vol. 9, No. 8, 2072, (August 1994).

50. Oshita, Y., "Low Temperature P-Doped SiC Growth by Chemical Vapor Deposition Using CH_3SiH_3/PH_3 Gas," *J. Electrochem. Soc.*, Vol. 142, 1002, (1995).

51. Robertson, R., and Gallagher, A.J., *J. Chem. Phys.*, Vol. 85, 3623, (1986).

52. Gates, S. M., *Surf. Sci.*, Vol.195, 307, (1988).

53. Allendorf, M.D., and Outka, D. A., *Surf. Sci.*, Vol. 258, 177, (1991).

54. Conlin, R. T., and Gill, R. S., *J. Am. Chem.* Soc. Vol. 105, 618, (1983).

55. Bozso, F., Yates, J.T., Choyke, W. J., and Muehlhoff, L. J., *J. Appl. Phys.*, Vol. 57, 2771, (1985).

56. Bean, K. E., Glein, P. S., and Yeakley, R. L., *J. Electrochem. Soc.*, Vol. 114, 733, (1967).

57. Carter, G., Colligon, J. S., and He, Z., "Ion-Assisted Deposition of C-N and Si-C-N films," *Thin Solid Films*, Vol. 283, 90-96, (1996).

58. Roenigk, K. F., and Jensen, K. F., "Low Pressure CVD of Silicon Nitride," *J. Electrochem. Soc.*, Vol. 134, No. 7, 1777, (July 1987).

59. Kingon, A. I., Lutz, L. J., Liaw, P., and Davis, R.F., "Thermodynamic Calculations for the Chemical Vapor Deposition of Silicon Carbide," *Journal of the American Ceramic Society,* Vol. 66, No. 8, 558, (August 1983).

60. Jacobson, K.A., "Growth, Texture, and Surface Morphology of SiC Layers," *J. Electrochem. Soc.* Vol. 118, No. 6, 1001, (June 1971).

61. Sigel, G. H., Jr., *Optical Absorption of Glasses*, Academic Press, New York, (1977).

62. Parsons, G. N., Souk, J. H., and Batey, J., "Low Hydrogen Content Stoichiometric Silicon Nitride Films Deposited by Plasma-Enhanced Chemical Vapor Deposition," *J. Appl. Phys.* , Vol. 70, 1190, (August 1991).